BMC Microbiology

RESEARCH

Open Access

Studying the effect bio-based sensorns packaging based on magnetic fields extraction of phycocyanin on the shelf life of fish fillets infected with *Staphylococcus aureus*

Bahareh Nowruzi[1*], Mahshid Ghorbani[1], Maryam Ghane[2], Mahrokh Ashrafizadeh[1], Rojan Barandak[1] and Melika Targholizadeh[1]

Abstract

Fish and seafood are highly perishable commodities, necessitating innovative packaging solutions to mitigate microbial spoilage and extend shelf life. This study developed a bioactive nanocomposite biosensor incorporating phycocyanin (PC) a pigment extracted from *Neowestiellopsis persica* and functionalized under 30 and 60 Millitesla (mT) magnetic fields (MF) coated with nanochitosan (NCT)- Sodium Alginate (SA). Reaults showed that MF exposure enhanced PC purity and concentration by 1.04- and 1.12-fold, respectively ($p < 0.05$), compared to non-MF controls. Agar disk diffusion assays revealed a 1.12-fold (30 mT) and 1.15-fold (60 mT) increase in antibacterial activity against *Staphylococcus aureus*. Films containing 2% PC (T4) extended shelf life by 8 days under refrigeration, reducing thiobarbituric acid (TBA) and total volatile nitrogen (TVN) levels to 18.85 ± 0.39 mg MDA/kg and < 30 mg/100 g, respectively, over 15 days. Furthermore, T4 significantly suppressed microbial proliferation relative to lower-concentration treatments and controls ($p < 0.05$). These results demonstrate that MF-enhanced, 2% PC nanocomposites provide a sustainable, biodegradable solution for seafood preservation, effectively delaying spoilage and advancing innovative packaging technologies.

Clinical trial number

IR.IAU. SRB.REC.1403.225.

Keywords Biofilms, Polyvinyl alcohol/chitosan nanocomposite, Sea food, Cyanobacteria, Natural product, Microbial spoilage

*Correspondence:
Bahareh Nowruzi
bahare77biol@gmail.com
[1]Department of Biology, SR.C, Islamic Azad University, Tehran, Iran
[2]Department of Biology, Islamshahr Branch, Islamic Azad University, Islamshahr, Iran

Introduction

The worldwide need for premium food products is growing, making advanced packaging systems essential for maintaining freshness and safety. Third-generation packaging employs innovative materials that track spoilage processes while offering protective, communicative, containment, and user-friendly features. In contrast, second-generation solutions prioritize reducing environmental footprints. The latest innovative packaging technologies, such as those used in seafood, continuously assess product integrity and provide real-time alerts about quality concerns. These advancements aim to extend shelf life, bolster food safety, and ensure standards in hygiene, traceability, and freshness are met [1]. By slowing oxidation and microbial growth, these innovations extend the shelf life of perishable items, particularly fishery products like fish, which are highly prone to spoilage. This approach not only reduces reliance on conventional plastics but also improves food safety and quality through advanced preservation techniques [2].

Foodborne illnesses and food poisoning are frequently attributed to contamination by pathogenic bacteria. Among these, *Staphylococcus aureus* is one of the most prevalent bacterial pathogens. Studies indicate that *S. aureus* is responsible for more fatalities than acquired immune deficiency syndrome (AIDS), tuberculosis, and viral hepatitis combined [3]. The clinical significance of methicillin-sensitive *Staphylococcus aureus* (MSSA) strains has risen substantially [4].

Cyanobacteria are Gram-negative bacteria with a profound evolutionary history, being the only prokaryotes capable of oxygenic photosynthesis [5]. The remarkable diversity within this group of microorganisms is reflected not only in their morphological variability and adaptability to diverse habitats (freshwater, marine, and terrestrial) but also in their extensive chemical repertoire of bioactive natural products [6]. This metabolic versatility facilitates their survival in highly competitive ecological niches [7]. The genus *Neowestiellopsis*, originally described by Kabirnataj et al. (2018) from Mazandaran, Iran, belongs to the order Nostocales and family Hapalosiphonaceae [8].

Phycocyanin (PC), a dominant pigment in the cyanobacterial genus *Neowestiellopsis*, exhibits a blue hue with a light absorption range of 560–600 nanometers. During algal photosynthesis, light energy absorbed by phycoerythrin (PE) is transferred sequentially to PC and then to chlorophyll, underscoring PC's critical role in light-harvesting processes [9].

The stability of PC is influenced by multiple extrinsic and intrinsic factors, including temperature, light intensity, pH fluctuations, pressure, exposure to heavy metal cations, denaturants, water activity, glass transition temperature, and the rheological properties of the surrounding medium [10]. To mitigate these destabilizing effects, encapsulation technologies have been employed to entrap PC within micro or nanoscale particles [11]. Encapsulation typically involves the binding of PC to polysaccharides such as alginate, chitosan, or pectin via functional groups, forming a stabilized matrix through intermolecular interactions [12].

Nanoencapsulation has recently emerged as a critical advancement in enhancing the efficacy of bioactive and therapeutic supplements within the food industry [13]. The antibacterial mechanism of chitosan nanoparticles is multifaceted and varies between Gram-negative and Gram-positive bacteria due to structural differences in their cell walls and membranes. While chitosan nanoparticles generally exhibit stronger antibacterial activity against Gram-negative bacteria, some studies report heightened sensitivity in Gram-positive strains. This discrepancy may arise from the lipopolysaccharide-rich outer membrane of Gram-negative bacteria, which contains anionic groups (e.g., phosphate and pyrophosphate) that impart a more negatively charged cell surface compared to the peptidoglycan and teichoic acid layers of Gram-positive bacteria. This structural distinction explains why chitosan nanoparticles induce more pronounced leakage of intracellular contents in Gram-negative bacteria than in Gram-positive species [14].

Recent studies demonstrate the superior efficacy of chitosan nanoparticles over unmodified chitosan. For instance, a two-hour incubation with chitosan nanoparticles significantly reduced *S. aureus* colony-forming units (CFUs), whereas four hours were required to achieve comparable results with chitosan alone. Similar trends were observed for *S. xylosus*. Furthermore, increasing chitosan nanoparticle concentrations markedly reduced the survival of *S. mutans* cells after 3 and 18 h of incubation. Most antibacterial assays involving chitosan and its derivatives are conducted during the late logarithmic growth phase of bacterial cultures [15].

MFs promote microalgal growth and modulate antioxidant defense systems, thereby enhancing cellular protection. For instance, exposure to a static MF (37.7–44.3 mT) induced structural reorganization of the thylakoid network in the cyanobacterium *Synechocystis aquatilis*, altering thylakoid membrane distribution and interthylakoid spacing. These effects are contingent on the specific parameters of the applied MF (e.g., static vs. oscillating, intensity, duration) [16].

Although MF applications in biological systems are regarded as novel, non-toxic, cost-effective, and easy-to-implement technologies, their underlying mechanisms remain incompletely characterized. Observed biological responses exhibit nonlinear dependencies on cultivation parameters, such as field intensity, frequency, and exposure duration [17]. Growing global consumer awareness

of food safety, nutritional value, and compositional integrity has driven a marked preference for natural preservatives. Research demonstrates that bio-based sensor packaging functionalized with PC, a bioactive compound extracted from the cyanobacterium *Neowestiellopsis persica* exerts beneficial antioxidant and antimicrobial effects on fresh fish fillets. These properties position PC -enriched packaging as a cost-effective, scalable, and sustainable alternative to synthetic preservatives.

While prior research has investigated the antimicrobial properties of PC, this study introduces two key advancements absent in existing literature. First, it is the first to incorporate PC into bio-based, sensor-enabled packaging designed for refrigerated storage a critical gap in current applications. Second, we pioneer a MF assisted extraction method for PC, synergistically combined with active sensor packaging to simultaneously enhance food preservation efficacy and enable real-time shelf-life monitoring. This dual innovation represents a novel strategy to optimize both extraction efficiency and intelligent packaging functionality.

This study investigated the efficacy of bio-based sensor packaging integrated with magnetically extracted PC, a bioactive pigment derived from the cyanobacterium *Neowestiellopsis persica*, to extend the shelf life of *S. aureus* contaminated fish fillets under refrigerated storage conditions (4 ± 1 °C) over 15 days. Through comprehensive analysis of antimicrobial, physicochemical, mechanical, and sensory parameters, the research demonstrated the viability of this innovative technology as a sustainable alternative to conventional synthetic preservatives and petroleum-based plastics. The findings address pressing challenges in food safety and sustainability by proposing an eco-friendly solution that aligns with contemporary consumer preferences for natural, non-toxic preservation methods. The implementation of this technology holds promises for mitigating foodborne illnesses, reducing post-harvest waste, and advancing circular economy principles within the fisheries sector, thereby contributing to enhanced public health outcomes and environmental stewardship through reduced reliance on non-renewable resources.

Materials and methods

Chemicals

All chemicals used in this study were of analytical grade and purchased from the Hi-Media, Merck, and Sigma manufacturers.

Culture conditions of the cyanobacterial strain

Cyanobacterial strains *Neowestiellopsis persica* isolated from Cyanobacteria culture collection (CCC) of herbarium ALBORZ at the Science and Research Branch, Islamic Azad University, Tehran, were grown in modified liquid Z8 medium and illuminated (300 $\mathrm{m^{-2}\,s^{-1}}$) growth rooms at 28 ± 2 °C for 10–15 days, respectively [18]. Figure 1; Table 1 summerizs the overall Methods brifly.

Application of MFs to the cyanobacterium *Neowestiellopsis persica* and PC extraction

A study of static magnetic field (SMF) in assays with *Neowestiellopsis persica* was carried out with ferrite magnets that were applied around the culture for 1 h daily. Each magnet was at 180 °, 15 cm above the base of the culture vessels. *Two different models of magnetic magnets* with a mean intensity of 30 mT (150 × 50 × 10 mm) and 60 mT (50 × 50 × 25 mm) were applied to the cyanobacterial cells and then the cells were centrifuged and collected. Then, the effects of magnetic fields were compared with control cultures [18].

The extraction of PC was carried out as described by Nowruzi et al. [19]. Briefly, PC was extracted from 500 mL of homogenized log-phase (14-day-old) culture. The culture was centrifuged at 4,000 rpm to pellet the cells, and the pellet was subsequently washed with phosphate buffer (pH 7.2) and lyophilized. PC was extracted from freeze-dried algal biomass (2 g) suspended in 500 mL of sodium phosphate buffer (0.1 M, pH 7.2). Repeated freeze-thaw cycles (– 20 °C freezing and room-temperature thawing in darkness) were applied over a one-week period to facilitate extraction. The homogenate was centrifuged (10,000 rpm, 30 min, 25 °C), and the supernatant was subsequently lyophilized. The final lyophilized product was stored at – 20 °C for further analysis [20] (Fig. 2).

Spectrophotometric determination of PC concentration and purity

Absorbance spectra of PC were recorded using a UV-Vis spectrophotometer (Hitachi, Japan). Spectral measurements were performed across a wavelength range of 250–700 nm, with absorbance values standardized against urea concentrations (0–10 M). PC concentration and PC purity were calculated according to published methodologies using the following equations, derived from absorbance values at 615 nm (A_{615}), 620 nm (A_{620}), 652 nm (A_{652}), and 280 nm (A_{280}) [21].

$$PC\ concentration = \frac{[\boldsymbol{A}_{615} - 0.474 \times \boldsymbol{A}_{652}]}{5.34}$$

$$PC\ purity = \frac{\boldsymbol{A}_{620}}{\boldsymbol{A}_{280}}$$

Determination of inhibition zone diameter, MIC and MBC of PC

Antibacterial activity was assessed using an *S. aureus* suspension standardized to 1.0×10^{7} CFU/mL. The inhibition zone diameter was determined via agar disc diffusion

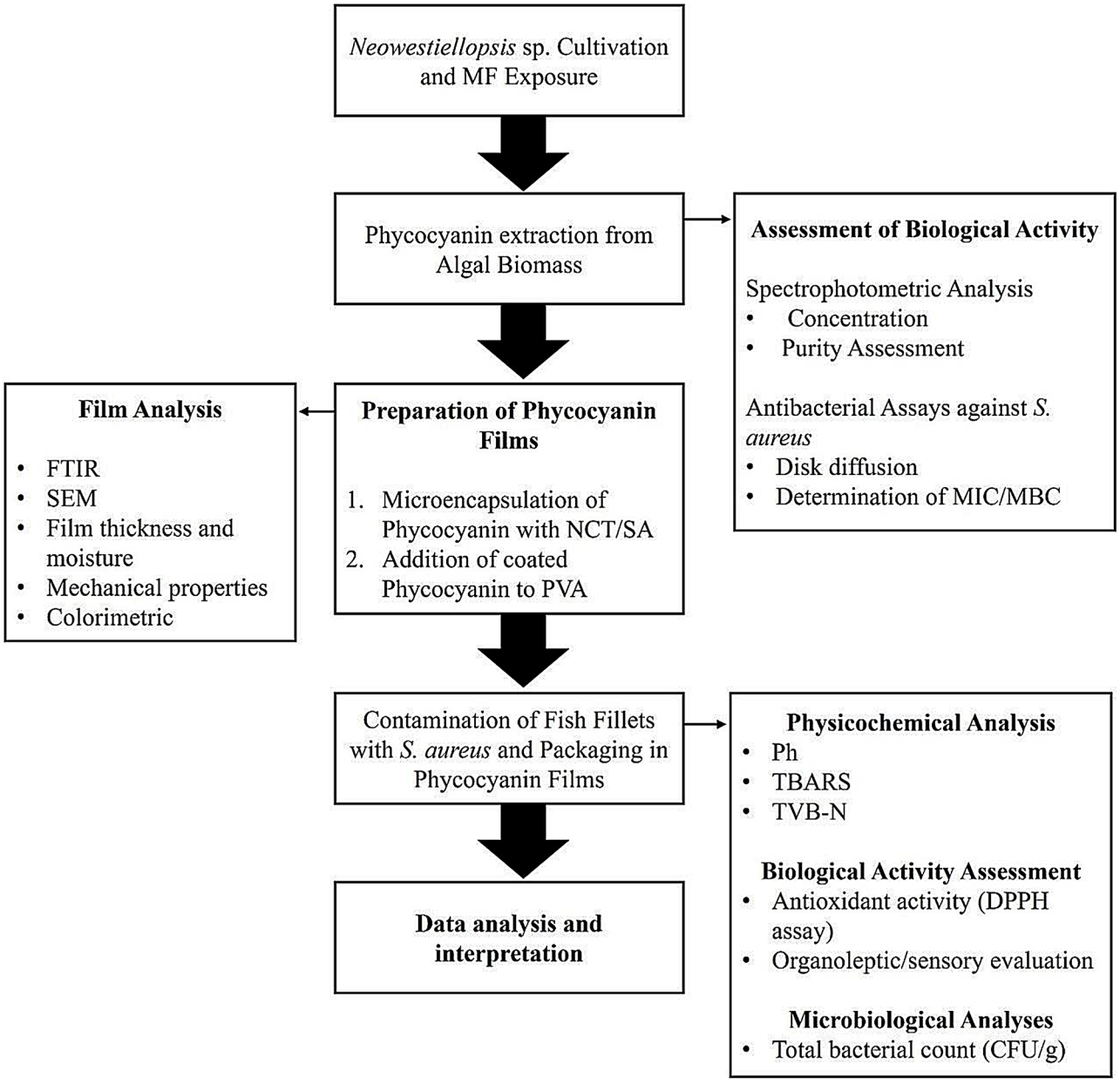

Fig. 1 Flowchart summarizing the methods briefly

assay, where PC was applied to sterile filter paper discs placed on inoculated agar plates. Following incubation at 37 °C for 24 h, inhibition zones were measured in triplicate and reported as mean diameter ± standard deviation (mm) [22].

To determine MIC and MBC, we used microdilution method. The lowest concentration that inhibited bacterial growth was defined as MIC. MBC was defined as the lowest concentration that caused complete death of the bacteria (99.9% reduction in CFU/mL) [23].

Coating of PC and Preparation of bio-based sensors

A 2% (w/w) solution of Nanochitosan (NCT) and a 2% (w/w) solution of Sodium Alginate (SA) were prepared. PC extract (1 mL) was gradually incorporated into the coating solution via dropwise addition. The mixture was homogenized at 10,000 rpm using a homogenizer (IKA, Germany). The resulting PC microparticle suspension was lyophilized [24]. 10% (w/w) aqueous polyvinyl alcohol (PVA) solution was prepared by dissolving 10 g of PVA powder in 90 mL of deionized water at 60 °C under continuous magnetic stirring for 30 min. Coated PC microparticles were added to the PVA matrix at final concentrations of 0%, 0.5%, 1%, and 2% (w/w) and homogenized

Table 1 Summary of processes for cyanobacterial culture, PC extraction, analysis, and sensor Preparation

Parameter	Specifications/Methods
Cyanobacterial culture	
Strain	*Neowestiellopsis persica* (CCC ALBORZ collection, Iran)
Growth medium	Modified liquid Z8 medium
Light intensity	300 µmol/m²/s
Temperature	28 ± 2 °C
Incubation period	10–15 days (log-phase harvested at 14 days)
Magnetic field (MF) exposure	
Intensity	30 mT and 60 mT (ferrite magnets)
Duration	1 h daily; magnets positioned 15 cm above culture vessels
Post-exposure processing	Centrifugation at 4,000 rpm for cell pelleting
PC extraction	
Biomass source	500 mL log-phase culture (14 days)
Centrifugation	4,000 rpm (cell pellet), 10,000 rpm (30 min, supernatant clarification)
Buffers	Phosphate buffer (pH 7.2), sodium phosphate buffer (0.1 M, pH 7.2)
Cell disruption	Repeated freeze-thaw cycles (– 20 °C freezing, room tempration thawing; 1 week)
Lyophilization	Supernatant lyophilized; stored at – 20 °C
Spectrophotometric analysis	
Instrument	UV-Vis spectrophotometer
Wavelengths	$\mathbf{A}_{615}$, $\mathbf{A}_{620}$, $\mathbf{A}_{652}$, $\mathbf{A}_{280}$
Standardization	Urea (0–10 M)
Antibacterial assays	
Test organism	*Staphylococcus aureus* (1.0× 10^7 CFU/mL)
Disc diffusion assay	Inhibition zone measured after 24 h at 37 °C (triplicate)
MIC/MBC determination	Microdilution method; MIC = lowest inhibitory concentration; MBC = 99.9% CFU reduction
Sensor preparation	
Coating agents	2% (w/w) (NCT), 2% (w/w) (SA)
Matrix solution	10% (w/w) (PVA) in deionized water (60 °C, 30 min stirring)
Plasticizer	15% (w/w) glycerol
Homogenization	10,000 rpm
Film formation	Casting in Petri dishes; drying at 25 ± 2 °C (48 h) followed by 50 °C (5 h)

at ambient temperature (25 ± 2 °C) for 60 min [25]. Glycerol (15% w/w) was subsequently introduced as a plasticizing agent [26].

For film formation, the composite solutions were cast into Petri dishes and dried at room temperature (25 ± 2 °C) for 48 h. Films were subsequently transferred to a drying oven at 50 °C for 5 h to complete solvent evaporation (Figs. 3 and 4) [25].

Indicator film tests

Fourier transform infrared spectroscopy (FTIR) analysis

The FTIR spectrum (Shimatzo, Japan) of the films was recorded using attenuated total reflection (ATR) in a smart FTIR method. Thin films were directly placed on the ZnSe ATR cell. For each spectrum, 64 consecutive scans were performed with a resolution of 4 cm^{-1} [27].

Scanning electron microscope (SEM) analysis

Film samples were sectioned into 2 × 2 cm in dimension and dissolved in glutaraldehyde and acetonitrile solvent. After attaching to the metal stubs and evaporating the solvent, the films were coated with gold in a Spatucker device under argon gas. The high electrical conductivity of gold and the enhancing effect of argon gas were used to optimize this process. Then, the samples were transferred to the SEM (Shimatzo, Japan) chamber. The particle size and their distribution in the coating were examined using electron bombardment and the signals obtained from the images [28].

Film thickness measurement

Film thickness was determined using a digital micrometer (Insize, China) with a precision of 0.001 mm. Measurements were recorded at three distinct locations per film to account for potential variability, and mean values were calculated for subsequent analyses [29].

Determination of moisture content

Film samples were sectioned into 4 × 4 cm squares, and their initial mass (M_i) was recorded using an analytical balance (Sartorius, Germany, ± 0.1 mg). The samples

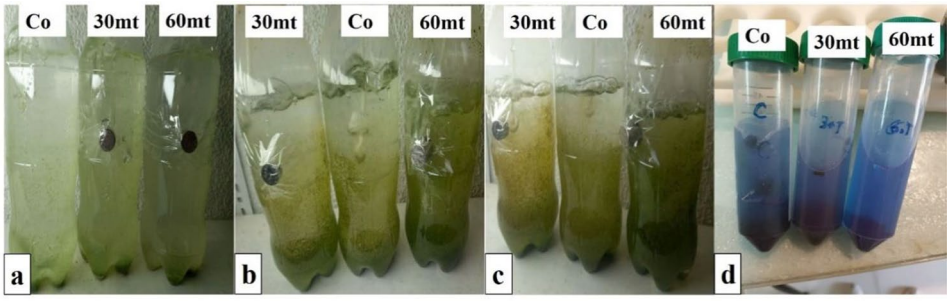

Fig. 2 Culture of cyanobacterium *Neowestiellopsis persica* in liquid Z8 medium for 14 days with magnets of 30 and 60 mT intensity. **a**) day 1, **b**) day 7, **c**) day 14, **d**) PC extracted by freeze-thaw method

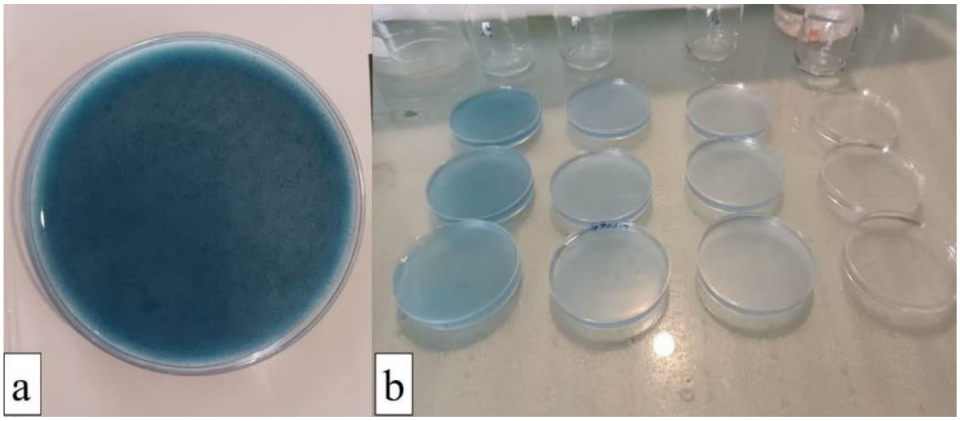

Fig. 3 Coating of PC **a**) PC nanoemulsion dried with SA and NCT **b**) Bio-Based Sensors prepared with different percentages of coated PC (0, 0.5, 1, and 2%)

were dried in an oven at 105 °C for 24 h and cooled immediately. After drying the samples, their weights were measured again (M_f) [30]. Moisture content (MC) was calculated as:

$$MC\ (\%) = \left(\frac{M_i - M_f}{M_i}\right) \times\ 100$$

where M_i is the initial mass (g) and M_f is the mass after drying (g).

Mechanical properties testing of films

The tensile properties of the films were evaluated using a texture analyzer (Brookfield, USA). Specimens were cut into 10 cm and preconditioned at 25 ± 1 °C and 50% relative humidity. Film thickness was measured at five randomly selected locations using a micrometer (Insize, China). Uniaxial tensile testing was performed with an initial grip separation of 50 mm and a crosshead speed of 50 mm/min. Tensile strength and elongation at break were calculated using the following equations [31]:

$$Elongation\ at\ break\ \% = \frac{Increase\ in\ length\ at\ break}{Initial\ length} \times 100$$

$$Tensile\ strength\ (MPa) = \frac{Maximum\ force}{Original\ cross - sectional\ area}$$

Colorimetric analysis (b, a*, L* values) of the films*

Film color parameters were quantified using a Hunter-Lab colorimeter (Hunter Lab, USA). The color indices L^* (lightness index), a^* (red-green index), and b^* (yellow-blue index) were identified to determine the color parameters of the samples [31].

Contamination of fish fillets with S. aureus

Fresh salmon fillets (Fig. 5) were surface-inoculated by immersion in a 0.5 McFarland standard suspension of *S. aureus* (PTCC 1917) prepared in Mueller-Hinton broth (MHB) for 20 s. PC treatment concentrations were selected based on prior MIC assays. Inoculated fillets were subsequently immersed in 80 mL of PC solution (Table 2) for 20 min, transferred to sterile polyethylene bags, and stored at 4 °C. Microbiological and chemical analyses were performed on days 1, 5, 10, and 12 post-treatment. Treated fillets were then vacuum-sealed in nanocomposite biofilms (Table 2). All experiments were conducted in triplicate ($n = 3$) to ensure statistical validity [32].

Tests for fish packaged in nanocomposites

pH measurement

The pH of homogenized fish samples was determined using a pH meter (Motorhome, Switzerland) at 25 ± 1 °C [33].

Measurement of thiobarbituric acid reactive substances (TBARS)

Lipid oxidation was assessed by quantifying TBARS using a spectrophotometric method. Briefly, 10 g of homogenized fish tissue was mixed with 5 mL of 4% (w/v) perchloric acid and 35 mL of 10% (w/v) trichloroacetic acid in a 50 mL Falcon tube. The mixture was centrifuged, and 2 mL of the supernatant reacted with 2 mL of 0.02 M TBA solution. The reaction mixture was incubated in a boiling water bath (100 °C) for 60 min, cooled to room temperature, and absorbance was measured at 500 nm using a UV-Vis spectrophotometer (Hitachi, Japan). TBARS values were expressed as mg malondialdehyde per kg sample [33].

Measurement of total volatile basic nitrogen (TVB-N)

The total volatile basic nitrogen (TVB-N) values were measured with a Kjeldahl flask (Ara Tajhiz, Iran), 10 g of the fish sample and 2 g of magnesium oxide were placed in a Kjeldahl flask. Then, 200 ml of distilled water was

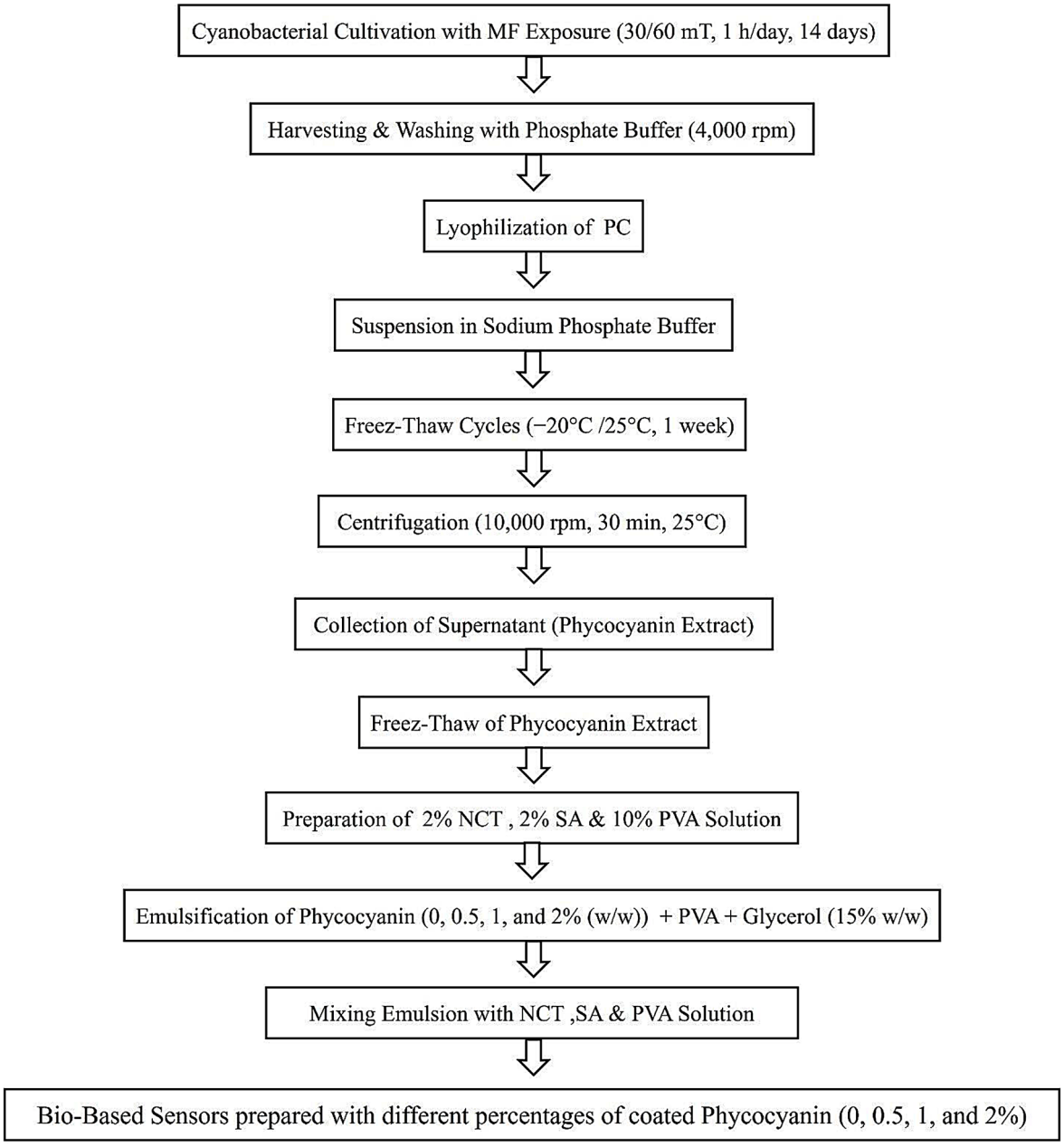

Fig. 4 Flowchart of the phycocyanin isolation, extraction, and bio-based sensors preparation

added. The flask was connected to the distillation apparatus. The distillate was collected in a flask containing a 2% (w/v) aqueous boric acid solution and a mixture of methyl red and bromocresol green indicators (each at 0.1%) in ethanol. The boric acid solution was titrated with 0.1 N sulfuric acid. TVB-N values were expressed in units of mg nitrogen Kg^{-1} (mg N Kg^{-1}) sample. Was calculated based on sulfuric acid consumption using the following formula [34]:

$$TVB-N\left(mg\frac{N}{100\,g}\right)=\frac{V\times\ 0.14\times\ 1000}{100}$$

where V = volume (mL) of H_2SO_4 consumed during titration.

Antioxidant activity measurement using the DPPH method

The free radical scavenging capacity of PC was evaluated using the 2,2-diphenyl-1-picrylhydrazyl (DPPH) (Merck, Germany) assay. Briefly, 1 mL of PC extract was combined with 1 mL of 0.002% (w/v) DPPH methanolic solution (0.1 mM) in a light-protected vial. The mixture was

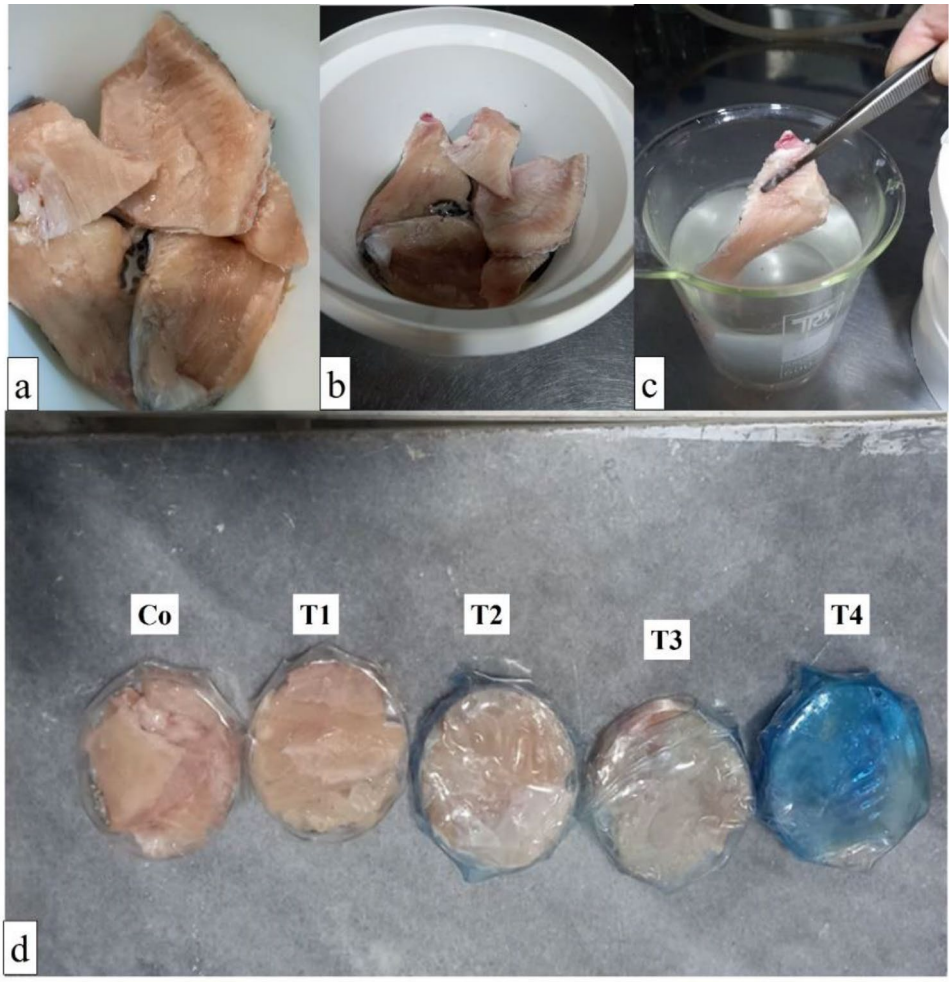

Fig. 5 Preparation and contamination stages of fish fillets with *S. aureus*. **a**) Collection of fish fillets **b**) Contamination of fish fillets with *S. aureus* suspension **c**) Coating contaminated fillets with different concentrations of PC **d**) Packaging contaminated fish fillets with nanocomposite biofilms. Healthy fish fillet (Co), Contaminated fish fillet packaged with bio-film without PC (T1), Contaminated fish fillet packaged with 0.5% (T2), 1% (T3) and 2% (T4) coated PC

Table 2 Classification of packaging formulations for fish fillets with different concentrations of films. Nanochitosan / Polyvinyl alcohol / Glycerol/ / sodium alginate/ phycocyanin films (NCT/PVA/G/SA/PC)

Treatment code	Formulation
Co	Control sample (fish fillet packaged in nanocomposite (NCT/PVA/G/SA)
T1	Fish fillet contaminated with *S. aureus* packaged in nanocomposite (NCT/PVA/G/SA)
T2	Fish fillet contaminated with *S. aureus* packaged in nanocomposite (NCT/PVA/G/SA) + 0.5% coated PC
T3	Fish fillet contaminated with *S. aureus* packaged in nanocomposite (NCT/PVA/G/SA) + 1% coated PC
T4	Fish fillet contaminated with *S. aureus* packaged in nanocomposite (NCT/PVA/G/SA) + 2% coated PC

incubated in darkness at 25 ± 2 °C for 30 min, and absorbance was measured at 517 nm. Ascorbic acid served as the positive control. Radical scavenging activity (%) was calculated as:

$$Inhibition\ (\%) = \left(\frac{A_{control} - A_{sample}}{A_{control}}\right) \times\ 100$$

where $A_{control}$ is the absorbance of the DPPH solution without PC and A_{sample} is the absorbance of the test mixture. Results were expressed as ascorbic acid equivalents (µg/mL) [35].

Evaluating the organoleptic properties

The sensory properties of fish fillets were examined based on a 5-point hedonic scale by 10 trained panelists. These properties included aroma, color, texture, and overall acceptance [36].

Microbiological analyses

Sample preparation

Ten grams of the sample were measured in a sterile plastic container. Sterile Peptinum buffer water was added in a 9:1 ratio to the sample weight. The mixture was homogenized using a Stomacher with sterile bags according to the Iranian National Standard No.9899. Then, 1 mL of the initial suspension was transferred into a tube containing 1 mL of diluent solution using a sterile pipette. Then, it was mixed for 5 to 10 s using a vortex (dilution 10^{-2}). When necessary, this process was repeated to get other dilutions [37].

Counting of total psychrotrophic bacteria

Aliquots (1 mL) of appropriate dilutions were spread-plated onto nutrient agar (Q-Lab, Canada) and incubated at 6.5 ± 0.5 °C for 10 days under aerobic conditions. Colonies were enumerated, and results were expressed as log (CFU/g) [38].

Counting of total viable mesophilic bacteria

Aliquots (0.1 mL) of homogenate dilutions were spread-plated on plate count and incubated at 30 ± 1 °C for 24 h. Plates containing 150 colonies were counted, and results were reported as log CFU/g [39].

Counting of enterobacteriaceae bacteria

One mL of homogenate dilutions was mixed with 10 to 15 mL of tempered (45 ± 1 °C) VRBGA culture medium (Q-Lab, Canada). The agar was gently swirled in figure-eight motions to ensure homogeneity and allowed to solidify. Plates were incubated at 37 ± 1 °C for 24 h. Characteristic pink-purple colonies with halos were enumerated, and results were expressed as log CFU/g [40].

Counting of S. aureus

Aliquots (1 mL) were combined with 10 to 15 mL of tempered (45 ± 1 °C) Baird Parker Agar (**BPA**) culture medium (Q-Lab, Canada) supplemented with egg yolk tellurite emulsion. After figure-eight mixing and solidification, plates were incubated at 37 ± 1 °C for 24 h. Colonies exhibiting shiny black halo morphology with clear zones were counted as presumptive *S. aureus* and reported as log CFU/g [40].

Statistical analysis

The data were reported as mean ± standard deviation and analyzed for one-way analysis of variance (ANOVA) by using SPSS (26.0, SPSS Statistical Software, Inc., USA). The differences between means were carried out by Duncan's multiple range test ($p < 0.05$).

Results

Spectroscopic analysis, purity, and concentration of PC extracted from *Neowestiellopsis persica*

The spectroscopic profile of PC extracted from *Neowestiellopsis persica* under standard and MF-treated growth conditions is illustrated in Fig. 6. Absorption maxima

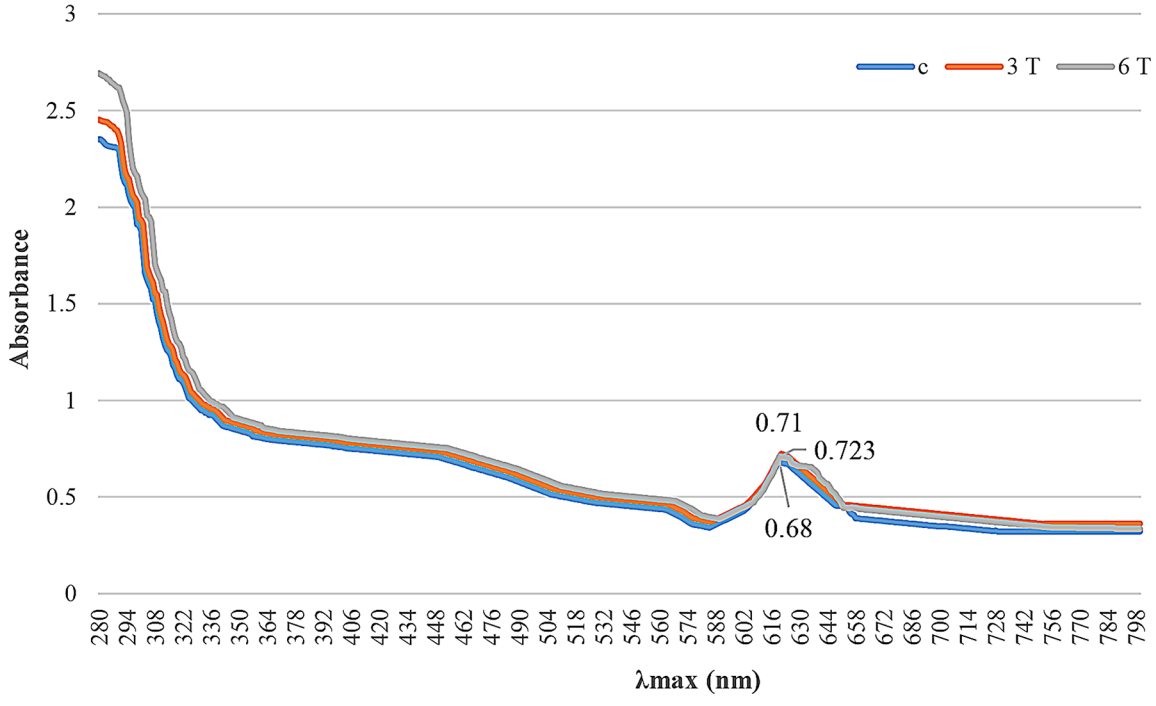

Fig. 6 Spectroscopic results of PC extracted from cyanobacteria grown under different conditions (Control and MFs of 30 mT and 60 mT)

Table 3 Results of the average growth Inhibition zone diameter (mm), MIC (mg/mL), and MBC (mg/mL) of PC grown under different conditions

	Co	30mT	60mT
Growth inhibition zone diameter (mm)	[b] 0.47 ± 10.66	[a] 0.81 ± 12.00	[a] 0.47 ± 12.33
MIC (mg/mL)	[a] 0.00 ± 5.00	[ab] 1.17 ± 4.16	[b] 1.17 ± 3.33

*Different lowercase letters show statistically significant differences in the row ($p < 0.05$)

(λmax) at 620 nm were recorded as 0.723, 0.68, and 0.71 for control, 30 mT MF, and 60 mT MF conditions, respectively. The highest absorption was observed in cultures exposed to a 30 mT MF.

Purity analysis revealed that PC extracted from *Neowestiellopsis persica* exposed to MFs exhibited a 1.02-fold increase (30 mT) and 1.06-fold increase (60 mT) in purity relative to the control ($p < 0.05$). Furthermore, elevating the MF intensity from 30 mT to 60 mT significantly enhanced purity values from 1.53 ± 0.00 to 1.59 ± 0.00 ($p < 0.05$).

PC concentration increased 1.12-fold in MF-treated cultures compared to the control ($p < 0.05$). However, no significant difference in concentration was observed when the MF intensity was increased from 30 mT to 60 mT ($p > 0.05$).

Antibacterial activity, MIC, and MBC of PC

The inhibitory effects of PC extracted from *Neowestiellopsis persica* under standard and MF-treated growth conditions are summarized in Table 3; Fig. 7. Exposure to a 30 mT MF resulted in a 1.12-fold increase in the inhibition zone diameter against *S. aureus* (0.81 ± 0.12 mm) compared to the control, while a 1.15-fold increase was observed at 60 mT (0.47 ± 0.12 mm) ($p < 0.05$). However, no significant difference in antibacterial activity was detected between 30 mT and 60 mT treatments ($p > 0.05$).

The minimum inhibitory concentration (MIC) of PC extracted from *Neowestiellopsis persica* under standard and MF-treated conditions is detailed in Table 3. Exposure to a 30 mT MF reduced the MIC by 0.83-fold (4.16 ± 0.30 mg/mL) compared to the control (5.00 ± 0.00 mg/mL), while a 0.66-fold reduction was observed at 60 mT (3.33 ± 1.17 mg/mL) ($p < 0.05$). However, increasing the MF intensity from 30 mT to 60 mT did not significantly alter the MIC value ($p > 0.05$). No minimum bactericidal concentration (MBC) against *S. aureus* was detected in any treatment ($p > 0.05$) (Table 3).

FTIR analysis results for identifying functional groups in biodegradable film

FTIR spectroscopy was employed to characterize functional groups and potential interactions in PVA films before and after incorporation of PC at varying concentrations (0.5%, 1%, and 2%). As illustrated in Fig. 8, the absorption bands of PC-loaded films exhibited spectra nearly identical to the control PVA film. Minor shifts in peak positions and intensities at specific wavenumbers were attributed to PC incorporation, suggesting weak physical interactions rather than chemical bonding.

Table 4 summarizes vibrational mode alterations under MF exposure. A reduction in O–H stretching vibration intensity was observed in treated samples. In contrast, the T3 sample exhibited increased intensities for asymmetric C–H, C = O, and C–C stretching vibrations, as well as C–O bending and C–N stretching modes, relative to the control. Similarly, the T2 sample showed enhanced bending vibrations for C–H, O–H, and N–H groups.

Morphological analysis via SEM

SEM revealed distinct morphological differences between biodegradable films. The control PVA film (Co) exhibited a smooth, crack-free surface. In contrast, the addition of coated PC (T1) induced the formation of wavy fibrous structures on the polymer matrix. As illustrated in Fig. 9, increasing the PC concentration to 1% (T2) and 2% (T3) further amplified the prominence of these wavy fibers.

Thickness results

Thickness analysis revealed no significant differences ($p > 0.05$) among biodegradable films across treatments, with all samples measuring 0.21 ± 0.01 mm.

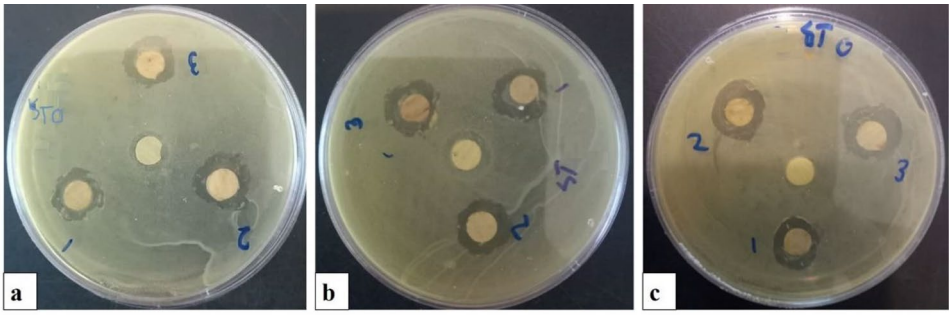

Fig. 7 Results of measuring the growth inhibition zone diameter under conditions of (**a**) Control, (**b**) 30 mT, and (**c**) 60 mT in three repetitions

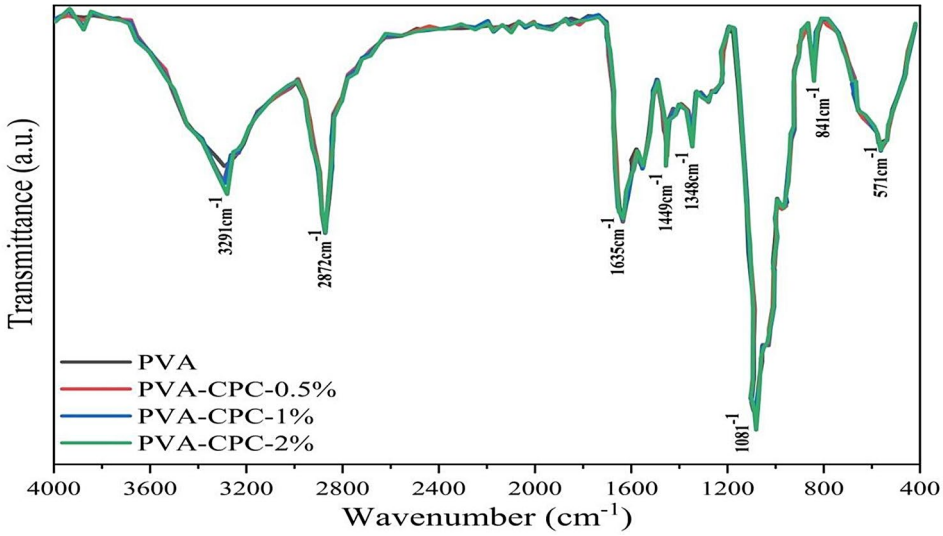

Fig. 8 FTIR spectra of biodegradable films of PVA with different percentages of PC

Table 4 Identification of functional groups and observed changes

Functional Group	Co	T1	T2	T3	Changes (Decrease - Increase) Compared to Control
O-H Stretching Vibrations	55.51	53.39293	53.13034	51.60894	Decrease
Asymmetric C-H Stretching	46.21	46.15738	46.19944	46.27547	Increase
C = O Stretching Vibrations	47.75	47.85358	48.00687	48.18935	Increase
C-H Bending Vibrations	59.10	61.91734	63.48924	62.70562	Increase
C-H Bending Vibrations	58.99	65.40272	65.76016	65.30374	Increase
C-O Bending Vibrations	20.55	25.00531	28.36906	28.77245	Increase
C-C Stretching Vibrations	58.75	60.83303	63.02258	68.34879	Increase
C = O Stretching Vibrations	47.75	47.85358	48.00687	48.18935	Increase
O-H Bending Vibrations	59.10	61.91734	63.48924	62.70562	Increase
N-H Bending Vibrations	58.99	65.40272	65.76016	65.30374	Increase
C-N Stretching Vibrations	20.55	25.00531	28.36906	28.77245	Increase

*Co: Control sample (PVA)/ T1: PVA + 0.5% coated PC / T2: PVA + 1% coated PC/ T3: PVA + 2% coated PC

Moisture content

As detailed in Table 5, the incorporation of coated PC significantly reduced moisture content compared to the control ($p < 0.05$). Increasing the PC concentration from 0.5% (13.01 ± 0.05%) to 2% (12.43 ± 0.07%) resulted in a 1.04-fold reduction in moisture ($p < 0.05$).

Mechanical properties

Tensile strength and elongation

As shown in Table 6, the tensile strength of biodegradable films significantly increased with the incorporation of coated PC compared to the control ($p < 0.05$). However, no statistically significant difference was observed when the PC concentration was elevated from 0.5 to 2% ($p > 0.05$).

Film elongation was significantly influenced by treatments ($p < 0.05$). The addition of coated **PC** reduced elongation compared to the control ($P < 0.05$), with a further decline observed at higher concentrations (0.5–2%, $p < 0.05$). The control sample exhibited the highest elongation, whereas the lowest value was recorded for the 2% PC film (T3, $p < 0.05$).

Color analysis

As summarized in Table 7, increasing the concentration of coated PC significantly reduced the brightness (L*), redness (a*), and yellowness (b*) of the biodegradable films compared to the control ($p < 0.05$). The 2% PC-loaded film (T3) exhibited 1.37-fold, 2.06-fold, and 1.77-fold reductions in L*, a*, and b* values, compared to the control respectively.

Antioxidant activity

As detailed in Table 8, the incorporation of coated PC significantly enhanced the antioxidant activity of the films compared to the control ($p < 0.05$). Increasing PC concentration from 0.5% (63.92 ± 1.07) to 2% (18.85 ± 0.39) resulted in a 3.39-fold increase in antioxidant capacity ($p < 0.05$). The highest activity was observed in the 2% PC

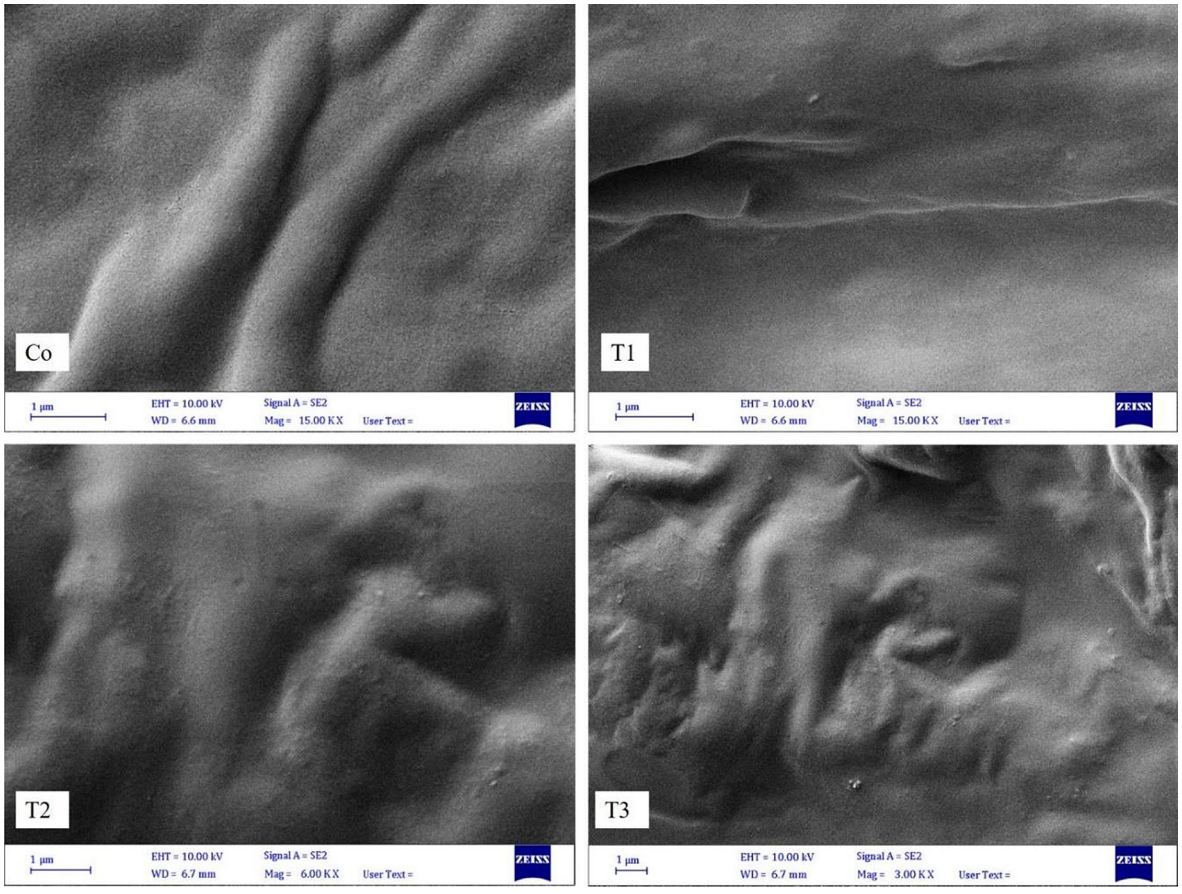

Fig. 9 Morphological analysis of the films (Co) Control sample (PVA) (T1) PVA and 0.5% coated PC, (T2) PVA and 1% coated PC (T3) PVA and 2% coated PC

Table 5 Moisture content results (%) for biodegradable films

	Co	T1	T2	T3
Moisture Content	13.56 ± 0.04^{a}	13.01 ± 0.05^{b}	12.81 ± 0.04^{c}	12.43 ± 0.07^{d}

* Co: Control sample (PVA)/ T1: PVA + 0.5% coated PC / T2: PVA + 1% coated PC / T3: PVA + 2% coated PC

* Different small and capital letters show significant differences within each column and row ($p < 0.05$)

Table 6 Results of tensile strength (N/cm^2) and elongation (%) of biodegradable films

	Co	T1	T2	T3
Tensile Strength (N/cm^2)	26.03 ± 0.58^{b}	29.98 ± 0.82^{a}	30.01 ± 0.62^{a}	29.54 ± 0.14^{a}
Elongation (%)	56.19 ± 0.79^{a}	56.09 ± 0.61^{a}	41.72 ± 0.19^{b}	35.31 ± 0.48^{c}

* Co: Control sample (PVA)/ T1: PVA + 0.5% coated PC / T2: PVA + 1% coated PC/ T3: PVA + 2% coated PC

* Different small and capital letters show significant differences within each column and row ($P < 0.05$)

Table 7 Average results of brightness index (L*), redness index (a*), and yellowness index (b*) of biodegradable films

	Co	T1	T2	T3
Brightness	97.12 ± 0.8^{a}	83.79 ± 0.19^{b}	79.32 ± 0.43^{c}	70.65 ± 0.60^{d}
Redness	10.82 ± 0.09^{a}	7.76 ± 0.13^{b}	6.32 ± 0.28^{c}	5.23 ± 0.15^{d}
Yellowness	25.40 ± 0.44^{a}	20.09 ± 0.78^{b}	17.39 ± 0.38^{c}	14.27 ± 0.25^{d}

* Co: Control sample (PVA)/ T1: PVA + 0.5% coated PC / T2: PVA + 1% coated PC / T3: PVA + 2% coated PC

* Different small and capital letters show significant differences within each column and row ($p < 0.05$)

Table 8 Antioxidant activity results (Ic50 = mg/mL) of biodegradable films

	Co	T1	T2	T3
Anti-oxidant activity	636.94 ± 46.68^{a}	63.92 ± 1.07^{b}	44.04 ± 0.41^{b}	18.85 ± 0.39^{b}

* Co: Control sample (PVA)/ T1: PVA + 0.5% coated PC / T2: PVA + 1% coated PC / T3: PVA + 2% coated PC

* Different small and capital letters show significant differences within each column and row ($p < 0.05$)

film (T3), while the lowest activity corresponded to the unmodified control ($p < 0.05$).

Results of fish fillets coated with biodegradable film

pH

As summarized in Table 9, contamination significantly increased the pH of fish fillets compared to the control ($p < 0.05$). However, packaging contaminated fillets with biodegradable films containing coated PC effectively mitigated this pH increase ($p < 0.05$). Notably, fillets coated with 2% PC (T4) exhibited the lowest pH among all treatments ($p < 0.05$), while those coated with the lowest PC concentration (T1) showed the highest pH by the 15th day of storage ($p < 0.05$).

TBA and TVB-N levels

The average TBA and TVB-N values for fish fillets during 15 days of storage are presented in Table 10. Both treatment type and storage duration significantly influenced TBA and TVB-N levels ($p < 0.05$). No significant differences were observed between groups at day 0 ($p > 0.05$); however, divergences emerged by day 3 ($p < 0.05$). Contamination significantly elevated TBA and TVB-N levels compared to the control ($p < 0.05$), while packaging contaminated fillets with PC-coated composites effectively mitigated these increases ($p < 0.05$). By day 15, T4 exhibited the lowest TBA and TVB-N values, whereas T1 displayed the highest ($p < 0.05$).

TBA levels in all treatments remained within national regulatory limits until day 7. Only T3 and T4 complied with standards through day 15, extending fillet shelf life by 8 days. In contrast, TVB-N levels for all treatments remained within approved thresholds throughout the 15-day storage period.

Microbial analysis

Mean bacterial counts (psychrotrophic, mesophilic, Enterobacteriaceae, and *S. aureus*) for fish fillets during storage are detailed in Table 11. Both treatment type and storage duration significantly influenced microbial proliferation ($p < 0.05$). No significant differences were observed in bacterial counts at day 0 ($p > 0.05$); however, divergences emerged by day 3 for all microbial groups ($p < 0.05$). A significant upward trend in psychrotrophic, mesophilic, Enterobacteriaceae, and *S. aureus* counts was observed across all treatments over 15 days ($p < 0.05$).

Packaging contaminated fillets with PC-coated composites (T4) significantly inhibited psychrotrophic, mesophilic, Enterobacteriaceae, and *S. aureus* growth ($p < 0.05$), with efficacy increasing proportionally to PC concentration. By day 15, T4 exhibited the lowest bacterial counts, while T1 displayed the highest ($p < 0.05$).

According to national standards for the count of psychrotrophic bacteria, only sample T4 was approved until day 3. For the number of mesophilic bacteria (log cfu/g), samples T2 and T3 were approved until day 3,and sample T4 was approved until day 7. For the count of Enterobacteriaceae, all samples were approved on day 1. For the count of *S. aureus* (log cfu/g), only the control sample was approved until day 7 and T4 was approved until day 3 according to the standard.

Table 9 Results of pH levels of fish fillet samples coated with biodegradable film during 15 days of storage

Day 15	Day 7	Day 3	Day 0	Day Tretment
^{Ab} 0.02 ± 6.71	^{Bb} 0.02 ± 6.21	^{Cc} 0.02 ± 5.78	^{Da} 0.03 ± 5.20	Co
^{Aa} 0.02 ± 6.91	^{Ba} 0.03 ± 6.46	^{Cb} 0.02 ± 6.07	^{Da} 0.04 ± 5.20	T1
^{Ab} 0.02 ± 6.70	^{Bb} 0.02 ± 6.20	^{Ca} 0.02 ± 5.98	^{Da} 0.02 ± 5.22	T2
^{Ac} 0.02 ± 6.60	^{Bc} 0.02 ± 6.12	^{Cc} 0.01 ± 5.80	^{Da} 0.03 ± 5.22	T3
^{Ad} 0.02 ± 6.41	^{Ad} 0.01 ± 5.98	^{Ad} 0.02 ± 5.74	^{Aa} 0.02 ± 5.20	T4

* Co: Control sample (PVA)/ T1: PVA + 0.5% coated PC / T2: PVA + 1% coated PC / T3: PVA + 2% coated PC

* Different small and capital letters show significant differences within each column and row ($p < 0.05$)

Table 10 Results of TBA (ppm) and TVB-N (mg/100 g) levels in fish fillet samples coated with biodegradable films during 15 days of storage

Day 15	Day 7	Day 3	Day 0	Day Treatment
TBA (ppm)				
^{Ac} 0.01 ± 1.03	^{Bc} 0.00 ± 0.56	^{Cc} 0.01 ± 0.47	^{Da} 0.01 ± 0.33	Co
^{Aa} 0.01 ± 1.21	^{Ba} 0.02 ± 0.76	^{Ca} 0.01 ± 0.59	^{Da} 0.01 ± 0.33	T1
^{Ab} 0.01 ± 1.14	^{Bb} 0.02 ± 0.68	^{Cb} 0.01 ± 0.52	^{Da} 0.04 ± 0.34	T2
^{Ad} 0.01 ± 0.92	^{Bd} 0.01 ± 0.51	^{Cd} 0.00 ± 0.40	^{Da} 0.03 ± 0.32	T3
^{Ae} 0.01 ± 0.73	^{Be} 0.02 ± 0.43	^{Ce} 0.01 ± 0.34	^{Da} 0.01 ± 0.30	T4
TVB-N (mg/100g)				
^{Ab} 0.43 ± 25.01	^{Bb} 0.43 ± 12.23	^{Cb} 0.43 ± 6.35	^{Da} 0.16 ± 1.03	Co
^{Aa} 0.28 ± 27.16	^{Ba} 0.16 ± 13.63	^{Ca} 0.28 ± 7.28	^{Da} 0.14 ± 0.98	T1
^{Ac} 0.58 ± 21.37	^{Bc} 0.28 ± 10.92	^{Cc} 0.56 ± 5.04	^{Da} 0.16 ± 1.03	T2
^{Ad} 0.58 ± 18.95	^{Bd} 0.28 ± 8.96	^{Cd} 0.21 ± 3.97	^{Da} 0.16 ± 1.03	T3
^{Ae} 0.43 ± 17.83	^{Be} 0.43 ± 7.09	^{Ce} 0.28 ± 2.80	^{Da} 0.08 ± 1.07	T4

*Co: Control sample (healthy fillet + PVA) / T1: Contaminated fillet + PVA / T2: Contaminated fillet + PVA + 0.5% coated PC / T3: Contaminated fillet + PVA + 1% coated PC / T4: Contaminated fillet + PVA + 2% coated PC

*Different lowercase and uppercase letters indicate statistical differences in each column and row ($p < 0.05$)

Table 11 Results of psychrotrophic bacteria count (log cfu/g), mesophilic bacteria count (log cfu/g), Enterobacteriaceae bacteria count (log cfu/g) and *S. aureus* (log cfu/g) in fish fillets coated with biodegradable films during 15 days of storage

Day 15	Day 7	Day 3	Day 0	Day Treatment
Psychrotrophic bacteria count (log cfu/g)				
^{Aa} 0.01 ± 9.39	^{Bb} 0.01 ± 8.34	^{Cb} 0.02 ± 6.31	^{Da} 0.02 ± 3.37	Co
^{Aa} 0.01 ± 9.42	^{Ba} 0.01 ± 8.41	^{Ca} 0.01 ± 6.44	^{Da} 0.00 ± 3.36	T1
^{Ab} 0.17 ± 9.15	^{Bc} 0.01 ± 8.30	^{Cb} 0.01 ± 6.29	^{Da} 0.03 ± 3.36	T2
^{Ac} 0.05 ± 8.69	^{Bd} 0.04 ± 7.83	^{Cc} 0.02 ± 6.03	^{Da} 0.02 ± 3.35	T3
^{Ad} 0.03 ± 7.92	^{Be} 0.02 ± 7.16	^{Cd} 0.01 ± 5.24	^{Da} 0.02 ± 3.35	T4
Mesophilic bacteria count (log cfu/g)				
^{Ad} 0.04 ± 10.05	^{Bc} 0.01 ± 8.26	^{Cd} 0.01 ± 7.35	^{De} 0.02 ± 4.26	Co
^{Aa} 0.01 ± 11.46	^{Ba} 0.01 ± 9.38	^{Ca} 0.01 ± 7.22	^{Da} 0.01 ± 5.39	T1
^{Ab} 0.03 ± 10.85	^{Bb} 0.02 ± 9.12	^{Cb} 0.04 ± 6.90	^{Db} 0.02 ± 5.18	T2
^{Ac} 0.01 ± 10.40	^{Bd} 0.01 ± 8.17	^{Cc} 0.04 ± 6.70	^{Dc} 0.02 ± 5.01	T3
^{Ae} 0.05 ± 9.68	^{Be} 0.03 ± 7.86	^{Ce} 0.01 ± 6.11	^{Dd} 0.02 ± 4.83	T4
Enterobacteriaceae bacteria count (log cfu/g)				
^{Aa} 0.01 ± 8.17	^{Ba} 0.03 ± 6.61	^{Ca} 0.01 ± 5.44	^{Da} 0.06 ± 2.66	Co
^{Ab} 0.02 ± 8.01	^{Bb} 0.01 ± 6.39	^{Cb} 0.04 ± 5.05	^{Da} 0.09 ± 2.65	T1
^{Ac} 0.00 ± 7.43	^{Bc} 0.02 ± 6.14	^{Cc} 0.01 ± 4.80	^{Da} 0.12 ± 2.63	T2
^{Ad} 0.01 ± 7.17	^{Bd} 0.01 ± 5.20	^{Cd} 0.01 ± 4.42	^{Da} 0.02 ± 2.59	T3
^{Ae} 0.04 ± 6.93	^{Be} 0.05 ± 4.94	^{Ce} 0.02 ± 4.21	^{Da} 0.16 ± 2.46	T4
(log cfu/g) *S. aureus*				
^{Ae} 0.04 ± 3.67	^{Be} 0.03 ± 2.86	^{Ce} 0.00 ± 0.00	^{Ce} 0.00 ± 0.00	Co
^{Ac} 0.02 ± 8.23	^{Ba} 0.01 ± 7.42	^{Ca} 0.01 ± 6.41	^{Da} 0.01 ± 5.25	T1
^{Ab} 0.02 ± 8.00	^{Bb} 0.03 ± 6.97	^{Cb} 0.03 ± 6.09	^{Db} 0.01 ± 5.04	T2
^{Ad} 0.01 ± 7.43	^{Bc} 0.05 ± 6.68	^{Cc} 0.03 ± 5.95	^{Dc} 0.04 ± 4.79	T3
^{Ad} 0.02 ± 6.92	^{Bd} 0.01 ± 6.12	^{Cd} 0.01 ± 3.30	^{Dd} 0.16 ± 4.32	T4

*Co: Control sample (healthy fillet + PVA) / T1: Contaminated fillet + PVA / T2: Contaminated fillet + PVA + 0.5% coated PC / T3: Contaminated fillet + PVA + 1% coated PC / T4: Contaminated fillet + PVA + 2% coated PC

*Different lowercase and uppercase letters indicate statistical differences in each column and row ($p < 0.05$)

Sensory evaluation of odor, texture, and color

Mean sensory evaluation scores for odor and texture of fish fillets during 15 days of storage are summarized in Table 12. Both treatment type and storage duration significantly influenced odor and texture scores ($p < 0.05$). No significant differences were observed between treatments at day 0 ($p > 0.05$); however, divergences emerged by day 3 ($p < 0.05$). Packaging contaminated fillets with PC-containing composites significantly improved sensory scores for odor and texture compared to the control and contaminated sample (T1) ($p < 0.05$). A significant decline in sensory quality occurred across all treatments over the 15-day storage period ($p < 0.05$). By day 15, T4 and T3 exhibited the highest sensory scores, while T1 scored the lowest ($p < 0.05$).

Results of color of fish fillets during 15 days of storage showed (Table 12), that treatment type and storage duration significantly influenced color scores ($p < 0.05$). No significant differences were observed between treatments at day 0 ($p > 0.05$); however, divergences emerged by day 3 ($p < 0.05$). Packaging contaminated fillets with PC-containing composites significantly improved color scores compared to the control and contaminated sample (T1) ($p < 0.05$). A significant decline in color scores occurred across all treatments over the storage period ($p < 0.05$), with no differences detected between groups by day 15 ($p > 0.05$).

Table 12 Sensory evaluation results for odor, texture and color of fish fillets coated with biodegradable film during 15 days of storage

Day 15	Day 7	Day 3	Day 0	Day Treatment
Evaluation results for odor				
^{Db} 0.00 ± 1.00	^{Cb} 0.00 ± 3.00	^{Ba} 0.00 ± 4.00	^{Aa} 0.00 ± 5.00	Co
^{Db} 0.00 ± 1.00	^{Cc} 0.00 ± 2.00	^{Bb} 0.00 ± 3.00	^{Aa} 0.00 ± 4.00	T1
^{Bb} 0.58 ± 1.33	^{Aab} 0.58 ± 3.33	^{Aa} 1.00 ± 4.00	^{Aa} 0.00 ± 4.00	T2
^{Ca} 0.58 ± 2.33	^{Bab} 0.58 ± 3.67	^{Aa} 0.58 ± 4.68	^{ABa} 0.00 ± 4.00	T3
^{Ca} 0.58 ± 2.33	^{Ba} 0.00 ± 4.00	^{Aa} 0.00 ± 5.00	^{Ba} 0.00 ± 4.00	T4
Evaluation results for texture				
^{Cc} 0.58 ± 1.33	^{Bb} 0.58 ± 2.67	^{Bb} 0.00 ± 3.00	^{Aa} 0.00 ± 5.00	Co
^{Dc} 0.00 ± 1.00	^{Cc} 0.00 ± 2.00	^{Bb} 0.00 ± 3.00	^{Aa} 0.00 ± 5.00	T1
^{Cbc} 0.58 ± 1.33	^{Ba} 0.58 ± 3.33	^{ABa} 0.00 ± 4.00	^{Aa} 0.00 ± 5.00	T2
^{Cab} 0.58 ± 1.33	^{Ba} 0.00 ± 3.33	^{Ba} 0.00 ± 4.00	^{Aa} 0.00 ± 5.00	T3
^{Ca} 0.58 ± 1.33	^{Ba} 0.00 ± 4.00	^{ABa} 0.58 ± 4.67	^{Aa} 0.00 ± 5.00	T4
Evaluation results for color				
^{Ca} 0.00 ± 1.00	^{Bbc} 0.58 ± 2.68	^{Bb} 0.00 ± 3.00	^{Aa} 0.00 ± 5.00	Co
^{Da} 0.00 ± 1.00	^{Cc} 0.00 ± 2.00	^{Bb} 0.00 ± 3.00	^{Aa} 0.00 ± 5.00	T1
^{Ca} 0.58 ± 1.33	^{Bab} 0.58 ± 3.33	^{ABab} 1.00 ± 4.00	^{Aa} 0.00 ± 5.00	T2
^{Ca} 0.58 ± 1.33	^{Bab} 0.58 ± 3.33	^{Bab} 0.00 ± 4.00	^{Aa} 0.00 ± 5.00	T3
^{Ca} 0.58 ± 1.33	^{Ba} 0.00 ± 4.00	^{ABa} 0.58 ± 4.67	^{Aa} 0.00 ± 5.00	T4

*Co: Control sample (healthy fillet + PVA) / T1: Contaminated fillet + PVA / T2: Contaminated fillet + PVA + 0.5% coated PC / T3: Contaminated fillet + PVA + 1% coated PC / T4: Contaminated fillet + PVA + 2% coated PC

*Different lowercase and uppercase letters indicate statistical differences in each column and row ($p < 0.05$)

Sensory evaluation of overall acceptability

Mean sensory evaluation scores for the overall acceptability of fish fillets during 15 days of storage are presented in Table 13. Both treatment type and storage duration significantly influenced overall acceptability ($p < 0.05$). No significant differences were observed between treatments

Table 13 Results of sensory evaluation for overall acceptability of fish fillet samples coated with biodegradable film during 15 days of storage

Day 15	Day 7	Day 3	Day 0	Day Treatment
^{Cb} 0.00 ± 1.00	^{Bbc} 0.58 ± 2.67	^{Bbc} 0.58 ± 3.33	^{Aa} 0.00 ± 5.00	Co
^{Db} 0.00 ± 1.00	^{Cc} 0.00 ± 2.00	^{Bc} 0.00 ± 3.00	^{Aa} 0.00 ± 4.00	T1
^{Ba} 0.00 ± 2.00	^{Aab} 0.58 ± 3.33	^{Aabc} 1.00 ± 4.00	^{Aa} 0.00 ± 4.00	T2
^{Ba} 0.58 ± 2.33	^{Aa} 0.58 ± 3.67	^{Aab} 0.58 ± 4.33	^{Aa} 0.00 ± 4.00	T3
^{Ba} 0.58 ± 2.67	^{Aa} 0.00 ± 4.00	^{Aa} 0.58 ± 4.67	^{Aa} 0.00 ± 4.00	T4

*Co: Control sample (healthy fillet + PVA) / T1: Contaminated fillet + PVA / T2: Contaminated fillet + PVA + 0.5% coated PC / T3: Contaminated fillet + PVA + 1% coated PC / T4: Contaminated fillet + PVA + 2% coated PC

*Different lowercase and uppercase letters indicate statistical differences in each column and row ($p < 0.05$)

at day 0 ($p > 0.05$); however, divergences emerged by day 3 ($p < 0.05$). Packaging contaminated fillets with PC-containing composites significantly improved overall acceptability compared to the control and contaminated sample (T1) ($p < 0.05$). A significant decline in acceptability occurred across all treatments over the storage period ($p < 0.05$), with T1 and the control exhibiting the lowest scores by day 15 ($p < 0.05$).

Results and discussion

Spectroscopic, purity, and concentration of PC

The application of MF to algae, microalgae, and cyanobacteria can influence metabolic activity, biomass synthesis, and the production of carbohydrates, pigments, essential amino acids, enzymes, and oxygen [41]. Notably, pigments extracted from cyanobacteria exposed to MF show promise as biosensors and biodegradable films for extending food shelf life.

In this study, the highest PC absorption (0.723 nm) was observed at an MF strength of 30 mT. This may reflect the accelerated entry of cyanobacterial cultures into the decline phase under 60 mT conditions, reducing biomass concentration after day 13. These findings align with Deamici et al. (2016), who reported a 57% increase in PC yield (13.17 mg/mL vs. 8.38 mg/mL in controls) in *Spirulina* sp. exposed to 60 mT MF for 1 h daily [16].

PC purity, assessed via the A_{620} and A_{280} ratio, is critical for determining commercial applicability. Ratios of 0.7–3.9 indicate food-grade quality [42]. Here, MF exposure significantly enhanced PC purity and concentration compared to untreated cultures [16].

Deamici et al. (2022) demonstrated that *Limnospira indica* cultures exposed to 11 mT MF (1 h/day) produced 123% more biomass than controls, with protein and chlorophyll content increasing to 60.4% (w/w) and 326%, respectively [43]. Similarly, Salari-Sichani et al. (2024) optimized MF-assisted PC extraction from *Spirulina platensis* (13.27 mT, 49.87 min, 17.11% solid-liquid ratio), achieving a 97.7% increase in concentration (5.44 mg/mL), 91.5% higher yield (26.34 mg/g), and 28.32% greater purity (24.32) compared to conventional methods [44]. These studies corroborate our findings that MF enhances PC yield and quality, underscoring its potential for scalable biotechnological applications.

PC, exhibits antibacterial properties against major Gram-positive and Gram-negative bacteria. Their antimicrobial action is initiated by electrostatic interactions between charged regions of bacterial cell walls/membranes and hydrophobic interactions with reactive moieties. These forces generate tension via Brownian motion in membrane macromolecules, leading to pore formation, membrane disintegration, leakage of intracellular contents (e.g., potassium ions), and eventual cell death [45]. Additionally, bioactive compounds in microalgal extracts disrupt membrane integrity by integrating hydrophobic molecules into phospholipid bilayers, further increasing permeability and cytoplasmic efflux [46].

Antibacterial activity, MIC, and MBC

Consistent with these mechanisms, our study demonstrated that PC extracted from *Neowestiellopsis persica* under 30 mT and 60 mT MFs exhibited enhanced antibacterial activity against *S. aureus* (reduced MIC, increased inhibition zones). Similar findings were reported by Safari et al. (2022), where pure and nanoencapsulated PC (maltodextrin/sodium caseinate composite) inhibited Gram-positive (*Listeria monocytogenes*, *S. aureus*, *Streptococcus iniae*) and Gram-negative (*Salmonella ruckeri*, *Escherichia coli*) pathogens [47]. Collectively, these studies highlight the dual role of MFs in boosting both PC yield and its functional potency.

FTIR

The incorporation of PC into PVA films increased peak intensity and induced a redshift (shift to lower wavenumbers) in FTIR absorption bands. PC contains hydroxyl (-OH) and amino (-NH) functional groups, whose overlapping vibrations enhance absorption intensity in this region. This suggests hydrogen bonding and electrostatic interactions between PC and the PVA matrix [48]. The observed redshift further confirms hydrogen bond formation, while reduced peak intensity at higher PC concentrations may reflect physicochemical interactions between the PE's aromatic rings and the polymer matrix. These interactions likely facilitate PC integration into PVA matrices, as evidenced by FTIR spectra. The minimal wavenumber shifts indicate that interactions are primarily physical (e.g., hydrogen bonding) rather than chemical [36].

Morphological

The SEM analysis revealed significant morphological changes in PVA films upon incorporating coated PC.

Pure PVA films (control) exhibited a smooth, homogeneous surface (Fig. 9), consistent with the strong hydrogen-bonding network characteristic of unmodified PVA matrices. In contrast, PC addition induced wavy fibrous structures on the film surface (T1), which became more pronounced at higher concentrations (T2, T3). This suggests concentration-dependent interactions between PVA and PC, likely driven by hydrogen bonding and partial self-aggregation of the PE, as observed in other natural colorant-polymer systems [49].

The increased surface roughness and fibrous morphology at higher PC loadings may indicate reduced polymer-pigment compatibility, consistent with studies on phase separation in PVA composites [50]. However, the absence of cracks or voids implies a semi-compatible system, where the PC interacts with PVA without fully disrupting the matrix. These morphological features could enhance biodegradability by increasing surface area for microbial action [51] but might compromise mechanical integrity [52].

Future work should explore strategies like plasticizers or pigment modification to optimize compatibility and correlate morphology with functional properties (e.g., barrier performance and biodegradation rates).

Thickness

Film thickness critically influences mechanical strength, water vapor permeability, light transmission, and opacity [53]. In this study, treatments had no significant effect on film thickness ($p > 0.05$), likely due to the low PC concentration and its compatibility with the PVA matrix [22]. Tie et al. (2024) reported similar consistency in carboxymethyl chitosan/pectin films (55–70 µm thickness) incorporating procyanidins and PC, attributing uniformity to dense network structures [54]. Conversely, Akhtar et al. (2024) observed increased thickness in edible films with 10% PC, suggesting concentration-dependent effects [24].

Moisture

Moisture sensitivity is a key consideration for food packaging, as excessive humidity absorption can compromise material functionality and product shelf life [55]. Here, PC incorporation significantly reduced film moisture content compared to controls ($p < 0.05$), likely due to hydrogen bonding between PC and the PVA matrix, which restricts free water mobility [56]. This contrasts with chitosan-based films, where hydrophilic properties often elevate moisture retention [57]. Similar trends were reported by Akhtar et al. (2024), who noted reduced moisture content, water solubility, and vapor permeability in SA/carboxymethyl cellulose films enriched with PC [24]. Chentir et al. (2019) further demonstrated that moisture content remained stable at PC concentrations ≤ 1.25% but declined at higher levels [58]., while Sun et al. (2023) observed analogous effects in curcumin-enhanced whey protein/cellulose nanocrystal films [59].

Mechanical properties

The mechanical properties of packaging materials are fundamental for ensuring food protection against environmental stressors. Key metrics such as tensile strength and elongation at rupture play a critical role in the design of biodegradable films, as these parameters determine the suitability of polymer-based layers for food packaging applications. A film's durability hinges on its ability to retain structural integrity when exposed to stresses during production, handling, and storage. The mechanical behavior of nanocomposite films is shaped by molecular bonding, compound solubility, and intermolecular forces within the polymer matrix. Incorporating specific additives can reconfigure the film's structural framework, strengthening interactions between components and improving overall performance [60].

In this study, PC incorporation significantly enhanced tensile strength compared to control films ($p < 0.05$), likely due to cross-linking between the pigment's functional groups and the polymer matrix. Conversely, elongation at break a measure of flexibility declined with PC addition ($p < 0.05$). These findings underscore the trade-off between mechanical robustness and pliability in bioactive films, emphasizing the need to optimize formulations for specific packaging requirements.

Color analysis

The incorporation of coated PC significantly reduced brightness (L*), redness (a*), and yellowness (b*) indices in biodegradable films compared to the control. The L*index (lightness: 100 = white, 0 = black) decreased with higher PC concentrations, reflecting increased opacity and darkness. This aligns with studies linking thicker or pigment-rich polymer layers to reduced brightness [61]. The a* index (redness: +120 = red, -120 = green) shifted toward green due to PC's natural blue-green hue, while the b* index (yellowness: +120 = yellow, -120 = blue) trended toward blue, consistent with PC's spectral properties. These shifts highlight PC's potential for tailoring film color toward blue-green spectra in food packaging.

Chentir et al. (2019) observed similar trends in gelatin- PC nanocomposites, where concentrations ≥ 6.5% reduced L* and increased opacity, enhancing light-blocking efficacy [58]. Nami et al. (2024) also discovered that adding PC nanoliposomes to a soy protein film matrix made the film less bright over time, with 20 g/100 g being the highest value seen [62]. Tie et al. (2024) further demonstrated that blending PC with PE in carboxymethyl chitosan/pectin films reduced brightness proportionally

to PE content, with analogous shifts in a* and b* values [54]. The study demonstrated significant changes in color indices (L*, a*, b*) of indicator biofilms during 14 days of storage, aligning with findings reported by Abed et al. (2025). Statistical analysis ($P < 0.05$) confirmed that control samples exhibited the highest brightness (L*), redness (a*), and yellowness (b*), while the incorporation of PC markedly reduced these values to 0.23, 0.88, and 0.89, respectively [63]. This reduction underscores PC's efficacy in modulating biofilm color properties, likely attributed to its natural pigmentation and synergistic interactions within the biofilm matrix. These results emphasize PC's potential as a functional additive for tailoring optical characteristics in biofilm-based systems, advancing strategies for optimizing color stability in food or biomedical applications.

Antioxidant activity

The incorporation of coated PC significantly enhanced the antioxidant activity of biodegradable films compared to control samples. PC, a phycobiliprotein, exhibits potent antioxidant properties attributed to its ability to scavenge alkoxyl (RO•), hydroxyl (•OH), peroxyl (ROO•), and peroxynitrite ($ONOO^-$) radicals, as well as neutralize hypochlorous acid (HOCl) under laboratory conditions [64].

Both apoprotein and phycocyanobilin—the chromophore moiety—contribute to this activity. The apoprotein inhibits •OH radicals via pH-dependent conformational changes and reacts with HOCl through cysteine and methionine residues, while phycocyanobilin neutralizes $ONOO^-$, HOCl, and ROO• via oxidation of its tetrapyrrole structure. During radical scavenging, PC undergoes spectral shifts, with absorption at 620 nm diminishing and new bands emerging near 640 nm [65]. Chitosan, a key polymer in the composite films, further augments antioxidant activity. Its amino groups form stable complexes with lipid oxidation byproducts (e.g., malondialdehyde), suppressing oxidative rancidity [66]. This synergy between PC and chitosan underscores the films' dual antioxidative mechanism: direct radical scavenging and inhibition of secondary oxidation pathways.

Chentir et al. (2019) demonstrated similar enhancements in gelatin- PC nanocomposites, where 12.5% PC (extracted from *Arthrospira* sp.) elevated chelation capacity, β-carotene bleaching inhibition, and DPPH radical scavenging by >40% compared to controls [58]. Akhtar et al. (2024) likewise reported dose-dependent antioxidant improvements in SA/carboxymethyl cellulose films enriched with PC [24].

Conversely, Tie et al. (2024) observed reduced activity in carboxymethyl chitosan/pectin films combining PC and fucoxanthin, likely due to competitive hydroxyl group interactions between pigments and the polymer matrix [54]. These findings highlight the importance of optimizing pigment-polymer compatibility to maximize antioxidative efficacy.

pH

Post-mortem fish pH typically ranges from 6.0 to 7.0, influenced by species, season, and spoilage-related biochemical changes [67]. In this study, PC-coated composites effectively stabilized fillet pH during 15-day storage, likely by inhibiting microbial growth and proteolytic activity that generate alkaline compounds (e.g., trimethylamine, ammonia) via protein degradation [68]. Similar mechanisms have been reported for chitosan-based coatings, where intrinsic antimicrobial properties suppress spoilage bacteria and enzymatic reactions, thereby delaying pH elevation [69]. Notably, all coated fillets remained consumable for 14 days, underscoring the dual antioxidant and antimicrobial efficacy of phycobiliproteins in preserving seafood quality [70].

Stejskal et al. (2020) demonstrated analogous pH stabilization in *Spirulina platensis*- PC gelatin films, attributing this to reduced microbial production of volatile amines [71]. Tavakoli et al. (2023) further corroborated these findings using smart films with cyanobacterial phycobiliproteins and anthocyanins, which slowed pH increases by >30% compared to controls [36]. Similarly, Nami et al. (2024) observed reduced pH drift in shrimp fillets coated with whey protein isolate containing PC nanoliposomes, linking this to inhibited trimethylamine accumulation [62].

TBA and TVB-N

Marine products, rich in omega-3 polyunsaturated fatty acids (PUFAs), are highly susceptible to lipid oxidation—a free-radical chain reaction (initiation, propagation, termination) that degrades sensory and nutritional quality [72]. Malondialdehyde (MDA), a secondary oxidation product derived from PUFA degradation, serves as a key marker in TBA assays. Its formation reflects advanced oxidative rancidity, as peroxides react with TBA to yield aldehydes and ketones [73]. PC's antioxidant properties likely mitigated lipid oxidation in coated fillets by scavenging free radicals (e.g., ROO•, •OH) and interrupting propagation stages. This aligns with studies showing that bioactive coatings reduce MDA accumulation by stabilizing lipid membranes and suppressing radical chain reactions [73].

Storage duration significantly influenced TBA values in fish fillets, with PC-containing composite films effectively suppressing lipid oxidation. This aligns with the well-documented oxygen barrier properties of such films, which limit oxidative attacks on polyunsaturated fatty acids (PUFAs) like docosahexaenoic acid (DHA) and eicosapentaenoic acid (EPA) [29, 74].

Chitosan, a key component of the coating, further contributed by scavenging free radicals (e.g., ROO•, •OH) via its amino groups, thereby slowing oxidation [69]. TBA values for all samples remained within acceptable limits (3–8 mg MDA/kg) throughout the 15-day storage period, consistent with standards for fresh and iced fish [75].

These findings corroborate studies demonstrating PC's antioxidative efficacy. Takyar et al. (2019) reported reduced lipid oxidation in refrigerated rainbow trout (*Oncorhynchus mykiss*) fillets coated with *Spirulina* extracts [76], while Stejskal et al. (2020) observed similar suppression in hake fillets using *Spirulina platensis*- PC coatings [71]. Seyedalangi et al. (2024) further highlighted synergistic effects between dielectric barrier discharge (DBD) plasma and PC, achieving > 40% greater TBARS reduction in combined treatments compared to individual applications [20]. This synergy underscores the potential of multifunctional coatings to enhance seafood preservation.

TVB-N remains a critical marker for assessing microbiological quality in fresh and minimally preserved seafood. Volatile bases, such as ammonia, trimethylamine, and methylamine, arise from enzymatic decarboxylation of amino acids post-mortem and correlate directly with microbial proliferation [77, 78].

In this study, storage duration significantly elevated TVB-N levels; however, PC-containing composite films effectively mitigated this increase. All samples complied with national standards (TVB-$N \leq 35$ mg/100 g) throughout the 15-day storage period. By day 15, fillets coated with 2% (T4) and 1% (T3) PC retained *excellent* quality (TVB-$N \leq 25$ mg/100 g), while controls (Co), T2 (0.5%), and contaminated T1 samples maintained *good* quality (TVB-$N \leq 30$ mg/100 g) [79].

Microbial analysis

This suppression aligns with chitosan's dual role in coatings: (1) inhibiting proteolytic bacteria and (2) disrupting microbial access to nitrogenous substrates [80]. PC further enhances this effect via antimicrobial and antioxidant mechanisms, delaying metabolite production [62]. For instance, Alparslan et al. (2019) reported reduced TVB-N in gelatin-orange essential oil-coated shrimp [81], while Özogul et al. (2021) observed similar trends in sardine fillets coated with microalgal PC [75]. Notably, Nami et al. (2024) documented slower TVB-N accumulation in shrimp coated with soy protein isolate- PC nanoliposomes, despite residual increases linked to enzymatic activity and bacterial spoilage [62]. These findings underscore the importance of optimizing PC concentration to balance microbial inhibition and structural compatibility.

Foodborne illnesses caused by *S. aureus* remain a global health concern, particularly in protein-rich seafood products where microbial proliferation is facilitated by proteolytic breakdown into amino acids [82]. In this study, PC -containing composites significantly inhibited *S. aureus* growth in contaminated fish fillets. This aligns with the antimicrobial mechanisms of microalgal extracts, which disrupt bacterial membrane integrity via hydrophobic and electrostatic interactions [46]. Chitosan, a cationic polymer in the composite, further enhanced this effect by binding to negatively charged microbial membranes through its NH_3^+ groups, inducing intracellular leakage and limiting oxygen permeability a critical factor in psychrotrophic bacterial suppression [69].

Notably, the 2% PC composite (T4) exhibited the strongest inhibition of psychrotrophic bacteria, *Enterobacteriaceae*, mesophiles, and *S. aureus*. This dose-dependent efficacy underscores PC's role as a functional additive, with higher concentrations (> 1%) achieving compliance with international standards for *S. aureus*-free seafood. Similar trends were reported by Mallikarjun Gouda et al. (2015), where *Spirulina platensis* extracts suppressed *S. aureus* and *E. coli* [83], and by Chentir et al. (2019), who observed broad-spectrum antimicrobial activity in PC -enhanced gelatin films [58]. Martínez-Antequera et al. (2021) further validated chitosan's preservative role in smoked fish fillets, demonstrating its ability to curb microbial growth [84].

Sensory evaluation of odor, texture and color

Sensory analysis revealed that PC composites preserved odor, color, texture, and overall acceptability of fish fillets, with T4 (2% PC) receiving the highest scores. This aligns with Baliti et al. (2020), who linked active seaweed extract coatings to reduced microbial spoilage and delayed browning in shrimp [85], and Nami et al. (2024), who reported improved organoleptic scores in PC-coated shrimp [62]. Similarly, Nowruzi et al. (2024) documented enhanced sensory quality in rainbow trout fillets coated with PC, attributing this to oxidative and microbial stability [86].

Sensory evaluation of overall acceptability

The superior sensory performance of high-concentration PC films (T4) likely stems from their dual antioxidative and antimicrobial properties, which mitigate spoilage volatiles (e.g., trimethylamine) and lipid oxidation byproducts. These findings mirror Tie et al. (2024), where carboxymethyl chitosan-pectin films with PC exhibited dose-dependent antimicrobial effects, though low concentrations (< 1%) paradoxically promoted bacterial growth [54].

Conclusion

This study evaluated the effects of MFs and NCT-SA-coated PC extracted from *Neowestiellopsis persica* on extending the shelf life of *S. aureus* contaminated fish fillets during 15 days of refrigerated storage. UV-Vis spectrophotometer analysis revealed that PC extracted under 30 mT and 60 mT MF exhibited absorbance maxima at 620 nm (0.68, 0.723, and 0.71, respectively), with the highest purity and concentration achieved at 30 mT. The PC demonstrated enhanced antibacterial activity against *S. aureus* under MF treatment, as evidenced by increased inhibition zone diameters and reduced minimum inhibitory/bactericidal concentrations (MIC/MBC). The 60 mT MF-treated PC, showing superior efficacy, was selected for incorporation into biodegradable films. FTIR spectroscopy confirmed the successful integration of PC into the PVA matrix via hydrogen bonding and electrostatic interactions. Morphological analysis revealed wavy fibrous structures in the polymer matrix, which intensified at higher PC concentrations (1–2%). While film thickness remained unaffected, moisture content decreased significantly ($p < 0.05$) with PC addition. Mechanical testing showed increased tensile strength but reduced elongation, indicating enhanced rigidity. Colorimetric analysis demonstrated dose-dependent reductions in lightness (L*) and shifts in redness (a*) and yellowness (b*) indices, aligning with PC's spectral properties. PCloaded films significantly improved antioxidant activity and suppressed spoilage markers in contaminated fillets: pH stabilization, reduced TBA values, and inhibited volatile nitrogen compound formation. Microbial analysis revealed suppressed growth of mesophilic, psychrotrophic, *Enterobacteriaceae*, and *S. aureus* populations. Sensory evaluation indicated that films with 2% PC (T4) maintained the highest acceptability (odor, color, texture) for 7 days, correlating with delayed oxidative and microbial spoilage. Overall, the T4 formulation extended fillet shelf life most effectively, underscoring the potential of MF-enhanced PC as a multifunctional bioactive agent in active food packaging.

Safety characteristics are necessary to evaluate NCT-SA-coated PC. In our study, we didn't evaluate the in vitro and in vivo safety of composites, due to the limitations in methodological standardization crucial to assessing their physiological benefits and health-promoting properties. Therefore, the saftly characterization of PC must be carried out through standard in vitro and in vivo experiments in the future. An important requirement for natural pigments is that they must be resistant to antimicrobials to ensure protection during therapeutic or preventive use while avoiding strains with acquired resistance that could limit effectiveness in human applications.

Acknowledgements
Not applicable.

Author contributions
Conceptualization, B.N, M.GH.; methodology, M.GH, M.GH; M.A; R.B.; M.T; software, B.N.; validation, B.N.; formal analysis, B.N. investigation, resources, B.N.

Funding
Not applicable.

Data availability
The datasets generated and/or analyzed during the current study are available in the datasets.

Declarations

Ethics approval and consent to participate
Not applicable.

Consent for publication
Not applicable.

Statement
All methods were conducted congruent with relevant guidelines and regulations. Authors done experiments on mouse tissue samples. All experimental protocols and panelists involved in the study were accepted by ethics committee of Tehran medical sciences, Islamic Azad University, Tehran, Iran (IR.IAU.SRB.REC.1403.225). This study is a clinical trial, we registered at Research ethics committees of Islamic Azad University -science and research branch, Date of Approval is 2024-06-08 and Approval ID is IR.IAU. SRB. REC.1403.225.

Live vertebrates and/or higher invertebrates
This study is not on live vertebrates and/or higher invertebrates.

Images
All the images are original and not copied from other papers. A clear statement on informed consent obtained from all the panelists.

Competing interests
The authors declare no competing interests.

Received: 14 February 2025 / Accepted: 17 April 2025
Published online: 02 May 2025

References

1. Ibrahim S, Fahmy H, Salah S. Application of interactive and intelligent packaging for fresh fish shelf-life monitoring. Front Nutr. 2021;8:677884.
2. Umaraw P, et al. Edible films/coating with tailored properties for active packaging of meat, fish and derived products. Trends Food Sci Technol. 2020;98:10–24.
3. Kourtis AP. Vital signs: epidemiology and recent trends in methicillin-resistant and in methicillin-susceptible Staphylococcus aureus bloodstream infections—United States. MMWR. Morbidity and mortality weekly report; 2019. p. 68.
4. Bouiller K, et al. Human infection of methicillin-susceptible Staphylococcus aureus CC398: a review. Microorganisms. 2020;8(11):1737.
5. Price GD, et al. Advances in Understanding the cyanobacterial CO2-concentrating-mechanism (CCM): functional components, ci transporters, diversity, genetic regulation and prospects for engineering into plants. J Exp Bot. 2008;59(7):1441–61.
6. Nowruzi B, et al. Nostoc cyanobacteria species: a new and rich source of novel bioactive compounds with pharmaceutical potential. J Pharm Health Serv Res. 2018;9(1):5–12.
7. Liu L, et al. Nostosins, trypsin inhibitors isolated from the terrestrial Cyanobacterium Nostoc Sp. strain FSN. J Nat Prod. 2014;77(8):1784–90.
8. Kabirnataj S, et al. Neowestiellopsis gen. Nov, a new genus of true branched cyanobacteria with the description of Neowestiellopsis persica Sp. Nov.

And Neowestiellopsis bilateralis Sp. Nov., isolated from Iran. Plant Syst Evol. 2018;304:501–10.
9. Lu W, et al. Antioxidant activity and healthy benefits of natural pigments in fruits: A review. Int J Mol Sci. 2021;22(9):4945.
10. Yuan B, et al. A review of recent strategies to improve the physical stability of phycocyanin. Curr Res Food Sci. 2022;5:2329–37.
11. Wang X, et al. Preparation of core-shell microcapsules based on microfluidic technology for the encapsulation, protection and controlled delivery of phycocyanin. J Drug Deliv Sci Technol. 2022;72:103361.
12. Park S, et al. Chitosan/cellulose-based porous nanofilm delivering C-phycocyanin: A novel platform for the production of cost-effective cultured meat. ACS Appl Mater Interfaces. 2021;13(27):32193–204.
13. Ghosh S, et al. Micro and nanoencapsulation of natural colors: A holistic view. Appl Biochem Biotechnol. 2021;193:3787–811.
14. Sotelo-Boyás M, et al. Physicochemical characterization of Chitosan nanoparticles and nanocapsules incorporated with lime essential oil and their antibacterial activity against food-borne pathogens. Lwt. 2017;77:15–20.
15. Orellano MS, et al. Chitosan nanoparticles enhance the antibacterial activity of the native polymer against bovine mastitis pathogens. Carbohydr Polym. 2019;213:1–9.
16. Deamici KM, Costa JAV, Santos LO. Magnetic fields as triggers of microalga growth: evaluation of its effect on Spirulina Sp. Bioresour Technol. 2016;220:62–7.
17. de Carvalho Silvello MA, et al. Microalgae-based carbohydrates: A green innovative source of bioenergy. Bioresour Technol. 2022;344:126304.
18. Eydelkhani M, Kiabi S, Nowruzi B. Vitro assessment of the effect of magnetic fields on efficacy of biosynthesized selenium nanoparticles by Alborzia Kermanshahica. BMC Biotechnol. 2024;24(1):27.
19. Nowruzi B, Anvar A, Ahari H. Extraction, purification and evaluation of antimicrobial and antioxidant properties of phycoerythrin from terrestrial Cyanobacterium Nostoc Sp. FA1. J Microb World. 2020;13(2):138–53.
20. Seyedalangi M, et al. The synergistic effect of dielectric barrier discharge plasma and phycocyanin on shelf life of Oncorhynchus mykiss rainbow fillets. Sci Rep. 2024;14(1):9174.
21. Antelo FS, Costa JAV, Kalil SJ. Purification of C-phycocyanin from Spirulina platensis in aqueous two-phase systems using an experimental design. Brazilian Archives Biology Technol. 2015;58(1):1–11.
22. Chen S, et al. Development of pH indicator and antimicrobial cellulose nanofibre packaging film based on purple sweet potato anthocyanin and oregano essential oil. Int J Biol Macromol. 2020;149:271–80.
23. Rezaei Savadkouhi N, Ariaii P, Charmchian M, Langerodi. The effect of encapsulated plant extract of hyssop (Hyssopus officinalis L.) in biopolymer nanoemulsions of Lepidium perfoliatum and Orchis mascula on controlling oxidative stability of soybean oil. Volume 8. Food Science & Nutrition; 2020. pp. 1264–71. 2.
24. Akhtar HMS, et al. Novel active composite films based on carboxymethyl cellulose and sodium alginate incorporated with phycocyanin: Physicochemical, microstructural and antioxidant properties. Food Hydrocolloids. 2024;147:109440.
25. Huang J, et al. Immobilization of roselle anthocyanins into Polyvinyl alcohol/hydroxypropyl Methylcellulose film matrix: study on the interaction behavior and mechanism for better shrimp freshness monitoring. Int J Biol Macromol. 2021;184:666–77.
26. Tarique J, Sapuan S, Khalina A. Effect of glycerol plasticizer loading on the physical, mechanical, thermal, and barrier properties of Arrowroot (Maranta arundinacea) starch biopolymers. Sci Rep. 2021;11(1):13900.
27. Jiang G, et al. Preparation and characterization of indicator films from carboxymethyl-cellulose/starch and purple sweet potato (Ipomoea Batatas (L.) lam) anthocyanins for monitoring fish freshness. Int J Biol Macromol. 2020;143:359–72.
28. Tongnuanchan P, Benjakul S, Prodpran T. Properties and antioxidant activity of fish skin gelatin film incorporated with citrus essential oils. Food Chem. 2012;134(3):1571–9.
29. Abdollahi M, et al. Comparing physico-mechanical and thermal properties of alginate nanocomposite films reinforced with organic and/or inorganic nanofillers. Food Hydrocolloids. 2013;32(2):416–24.
30. Naidu DS, John MJ. Effect of clay nanofillers on the mechanical and water vapor permeability properties of xylan–alginate films. Polymers. 2020;12(10):2279.
31. Alizadeh-Sani M, et al. pH-responsive color indicator films based on Methylcellulose/chitosan nanofiber and barberry anthocyanins for real-time monitoring of meat freshness. Int J Biol Macromol. 2021;166:741–50.
32. Rodríguez-Tudela JL, et al. Correlation of the MIC and dose/mic ratio of fluconazole to the therapeutic response of patients with mucosal candidiasis and candidemia. Antimicrob Agents Chemother. 2007;51(10):3599–604.
33. Bazargani-Gilani B. Activating sodium alginate-based edible coating using a dietary supplement for increasing the shelf life of rainbow trout fillet during refrigerated storage (4 ± 1 C). J Food Saf. 2018;38(1):e12395.
34. Li T, et al. Coating effects of tea polyphenol and Rosemary extract combined with Chitosan on the storage quality of large yellow croaker (Pseudosciaena crocea). Food Control. 2012;25(1):101–6.
35. Torruco-Uco J, et al. Angiotensin-I converting enzyme inhibitory and antioxidant activities of protein hydrolysates from Phaseolus lunatus and Phaseolus vulgaris seeds. LWT-Food Sci Technol. 2009;42(10):1597–604.
36. Tavakoli S, et al. Novel intelligent films containing anthocyanin and phycocyanin for nondestructively tracing fish spoilage. Food Chem. 2023;402:134203.
37. Mari A, Antonini G. Validation of the micro biological survey method for total viable count and E. coli in food samples. Am J Food Technol. 2011;6(11):951–62.
38. Raeisi S, et al. Evaluation of antioxidant and antimicrobial effects of Shallot (Allium ascalonicum L.) fruit and Ajwain (Trachyspermum ammi (L.) Sprague) seed extracts in semi-fried coated rainbow trout (Oncorhynchus mykiss) fillets for shelf-life extension. LWT-Food Sci Technol. 2016;65:112–21.
39. Rahman MA, et al. Isolation, identification and antibiotic sensitivity pattern of Salmonella spp. From locally isolated egg samples. Am J Pure Appl Sci. 2019;1(1):1–11.
40. Ramezani Z, Zarei M, Raminnejad N. Comparing the effectiveness of Chitosan and Nanochitosan coatings on the quality of refrigerated silver carp fillets. Food Control. 2015;51:43–8.
41. da Menestrino C. Magnetic fields exhibit a positive impact on lipid and biomass yield during phototrophic cultivation of Spirulina Sp. Bioprocess Biosyst Eng. 2021;44(10):2087–97.
42. de Amarante MCA, et al. Design strategies for C-phycocyanin purification: process influence on purity grade. Sep Purif Technol. 2020;252:117453.
43. Deamici KM, et al. Microalgae cultivated under magnetic field action: insights of an environmentally sustainable approach. Sustainability. 2022;14(20):13291.
44. Salari-Sichani B, Jahadi M, Nourani M. Magnetic-field-assisted extraction of phycocyanin from Spirulina platensis. Microchem J. 2024;206:111463.
45. Zarandi-Miandoab L et al. Phycocyanin, as a cyanobacterial antioxidant: structure, function and applications. J Plant Process Function, 2022(1): pp. 1–22.
46. Schuelter AR, et al. Isolation and identification of new microalgae strains with antibacterial activity on food-borne pathogens. Engineering approach to optimize synthesis of desired metabolites. Biochem Eng J. 2019;144:28–39.
47. Safari R, et al. Evaluation and comparison of antioxidant and antibacterial properties of phycocyanin extracted from spirulina algae (Spirulina Platensis) in both pure and nanoencasulated forms with maltodextrin-sodium caseinate combination coating. J Food Sci Technol (Iran). 2022;19(127):345–58.
48. Li S, et al. A green versatile packaging based on alginate and anthocyanin via incorporating bacterial cellulose nanocrystal-stabilized camellia oil Pickering emulsions. Int J Biol Macromol. 2023;249:126134.
49. Huang J, et al. Make your packaging colorful and multifunctional: the molecular interaction and properties characterization of natural colorant-based films and their applications in food industry. Trends Food Sci Technol. 2022;124:259–77.
50. Wardana AA, et al. The incorporation of Chitosan nanoparticles enhances the barrier properties and antifungal activity of Chitosan-based nanocomposite coating films. Int J Biol Macromol. 2024;280:135840.
51. Farrokheh A, Ahmadi Z. Biodegradable polymer films incorporating phycocyanin and polyhydroxybutyrate: advancing sustainable packaging technologies. Biodegradation. 2025;36(2):29.
52. Wang Y et al. Stability enhancement methods for natural pigments in intelligent packaging: a review. Crit Rev Food Sci Nutr, 2024: pp. 1–16.
53. Yong H, et al. Effects of anthocyanin-rich purple and black eggplant extracts on the physical, antioxidant and pH-sensitive properties of Chitosan film. Food Hydrocolloids. 2019;94:93–104.
54. Tie S, et al. Design and Preparation of novel antioxidant and antibacterial films containing procyanidins and phycocyanin for food packaging. RSC Adv. 2024;14(11):7572–81.
55. Leceta I, Guerrero P, De La Caba K. Functional properties of chitosan-based films. Carbohydr Polym. 2013;93(1):339–46.
56. Bergo P, Moraes ICF, Sobral PJdA. Effects of plasticizer concentration and type on moisture content in gelatin films. Food Hydrocolloids. 2013;32(2):412–5.

57. Lim H, Huang N, Loo C. Facile Preparation of graphene-based Chitosan films: enhanced thermal, mechanical and antibacterial properties. J Non-cryst Solids. 2012;358(3):525–30.
58. Chentir I, et al. Biofunctional gelatin-based films incorporated with food grade phycocyanin extracted from the Saharian Cyanobacterium Arthrospira Sp. Food Hydrocolloids. 2019;89:715–25.
59. Sun H, et al. Effects of Curcumin, phycocyanin, or modified lycopene colorants on the physicochemical and sensory properties of Whey protein–cellulose nanocrystal packaging films. Food Chem. 2023;412:135541.
60. Pereira PF, et al. Electrical gas sensors for meat freshness assessment and quality monitoring: A review. Trends Food Sci Technol. 2021;118:36–44.
61. Maruddin F et al. Brightness, elongation and thickness of edible film with caseinate sodium using a type of plasticizer. in IOP conference series: Earth and environmental science. 2020. IOP Publishing.
62. Nami B, et al. Development of soy protein isolate films incorporated with phycocyanin-loaded nanoliposomes to maintain shrimp freshness. LWT. 2024;196:115803.
63. Abed S, Nowruzi B, Anvar SAA. Production of Oncorhynchus mykiss biosensor based on Polyvinyl alcohol/chitosan nanocomposite using phycocyanin during refrigerated storage. Sci Rep. 2025;15(1):703.
64. Romay C, et al. C-phycocyanin: a biliprotein with antioxidant, anti-inflammatory and neuroprotective effects. Curr Protein Pept Sci. 2003;4(3):207–16.
65. Fernández-Rojas B, Hernández-Juárez J, Pedraza-Chaverri J. Nutraceutical properties of phycocyanin. J Funct Foods. 2014;11:375–92.
66. Muñoz-Tebar N, et al. Chitosan edible films and coatings with added bioactive compounds: antibacterial and antioxidant properties and their application to food products: a review. Polymers. 2023;15(2):396.
67. Stamatis N, Arkoudelos JS. Effect of modified atmosphere and vacuum packaging on microbial, chemical and sensory quality indicators of fresh, filleted Sardina pilchardus at 3 C. J Sci Food Agric. 2007;87(6):1164–71.
68. Abbas KA, et al. A review on correlations between fish freshness and pH during cold storage. Am J Biochem Biotechnol. 2008;4(4):416–21.
69. Yaghoubi M, et al. Effect of Chitosan coating incorporated with Artemisia Fragrans essential oil on fresh chicken meat during refrigerated storage. Polymers. 2021;13(5):716.
70. Haghdoost A, et al. Assessment of the potential of algae Phycobiliprotein nanoliposome for extending the shelf life of common carp burgers during refrigerated storage. Fisheries Aquat Sci. 2022;25(5):276–86.
71. Stejskal N, et al. Quality enhancement of refrigerated Hake muscle by active packaging with a protein concentrate from Spirulina platensis. Food Bioprocess Technol. 2020;13:1110–8.
72. Okpala COR, et al. Lipid oxidation kinetics of ozone-processed shrimp during iced storage using peroxide value measurements. Food Bioscience. 2016;16:5–10.
73. Shahidi F, Zhong Y. Lipid oxidation and improving the oxidative stability. Chem Soc Rev. 2010;39(11):4067–79.
74. Arora A, Padua G. Nanocomposites in food packaging. J Food Sci. 2010;75(1):R43–9.
75. Özogul İ, et al. The effects of microalgae (Spirulina platensis and Chlorella vulgaris) extracts on the quality of vacuum packaged sardine during chilled storage. J Food Meas Charact. 2021;15:1327–40.
76. Takyar MBT, Khajavi SH, Safari R. Evaluation of antioxidant properties of Chlorella vulgaris and Spirulina platensis and their application in order to extend the shelf life of rainbow trout (Oncorhynchus mykiss) fillets during refrigerated storage. Lwt. 2019;100:244–9.
77. Özoğul F, Özoğul Y. Comparision of methods used for determination of total volatile basic nitrogen (TVB-N) in rainbow trout (Oncorhynchus mykiss). Turkish J Zool. 2000;24(1):113–20.
78. Maghami M, Motalebi AA, Anvar SAA. Influence of Chitosan nanoparticles and fennel essential oils (Foeniculum vulgare) on the shelf life of Huso huso fish fillets during the storage. Volume 7. Food science & nutrition; 2019. pp. 3030–41. 9.
79. Ólafsdóttir G. Volatile compounds as quality indicators in chilled fish: evaluation of microbial metabolites by an electronic nose. Iceland: University of Iceland, Faculty of Science, Department of Food Science and Nutrition, Iceland and Icelandic Fisheries Laboratories, Reykjavik; 2005.
80. Huang J, et al. Functional characteristics improvement by structural modification of hydroxypropyl Methylcellulose modified Polyvinyl alcohol films incorporating roselle anthocyanins for shrimp freshness monitoring. Int J Biol Macromol. 2020;162:1250–61.
81. Alparslan Y, et al. The role of gelatin-based film coating combined with orange Peel essential oil on the quality of refrigerated shrimp. Acta Aquatica Turc. 2019;15(2):197–212.
82. Indumathi M, Sarojini KS, Rajarajeswari G. Antimicrobial and biodegradable Chitosan/cellulose acetate phthalate/zno nano composite films with optimal oxygen permeability and hydrophobicity for extending the shelf life of black grape fruits. Int J Biol Macromol. 2019;132:1112–20.
83. Mallikarjun Gouda K, Kavitha M, Sarada R. Antihyperglycemic, antioxidant and antimicrobial activities of the butanol extract from S pirulina platensis. J Food Biochem. 2015;39(5):594–602.
84. Martínez-Antequera FP, et al. Evaluation of the inclusion of the green seaweed Ulva Ohnoi as an ingredient in feeds for Gilthead sea Bream (Sparus aurata) and European sea bass (Dicentrarchus labrax). Animals. 2021;11(6):1684.
85. Balti R, et al. Active exopolysaccharides based edible coatings enriched with red seaweed (Gracilaria gracilis) extract to improve shrimp preservation during refrigerated storage. Food Bioscience. 2020;34:100522.
86. Nowruzi B, et al. Studying the impact of phycoerythrin on antioxidant and antimicrobial activity of the fresh rainbow trout fillets. Sci Rep. 2024;14(1):2470.

Publisher's note